

## Observed vertical redistribution of black carbon and other insoluble light-absorbing particles in melting snow

Sarah J. Doherty,<sup>1</sup> Thomas C. Grenfell,<sup>2</sup> Sanja Forsström,<sup>3</sup> Dean L. Hegg,<sup>2</sup> Richard E. Brandt,<sup>2,4</sup> and Stephen G. Warren<sup>2</sup>

Received 2 October 2012; revised 28 January 2013; accepted 30 January 2013.

[1] Light-absorbing impurities in snow reduce snow albedo, producing a positive radiative forcing, warming the surface air and snowpack, and accelerating snow melt. As the snow melts, black carbon (BC) and other insoluble light-absorbing particulate impurities (ILAP) are retained at the snow surface because their scavenging efficiency with meltwater is <100%, so concentrations of ILAP in surface snow increase with snow melt, further reducing snow albedo. The magnitude of this positive feedback depends on the scavenging efficiency of BC and other ILAP with snow meltwater. We present results from field measurements of the vertical distribution of BC and other ILAP in snow near Barrow (Alaska), the Dye-2 station in Greenland and Tromsø (Norway) during the melt season. Amplification factors due to melt are calculated for the concentrations in surface snow of BC and all ILAP. At Barrow and Dye-2, melt scavenging rates are estimated. Melt amplification appears generally to be confined to the top few centimeters of the snowpack, where it increases concentrations of BC and other ILAP by up to a factor of about five. Scavenging fractions of ILAP due to percolation of meltwater are estimated at 10–30%, with the rates for BC being comparable or a few percent lower. The lack of distinction may result from the particles in snow being internal mixtures of both BC and other ILAP, so that scavenging efficiencies for these internally mixed particles are determined by the total particle size and hydrophobicity rather than being different for individual particle components.

**Citation:** Doherty, S. J., T. C. Grenfell, S. Forsström, D. L. Hegg, R. E. Brandt, and S. G. Warren (2013), Observed vertical redistribution of black carbon and other insoluble light-absorbing particles in melting snow, *J. Geophys. Res. Atmos.*, 118, doi:10.1002/jgrd.50235.

### 1. Introduction

[2] Darkening of snow by insoluble light-absorbing particulates (ILAP) such as black carbon increases the absorption of solar radiation, leading to warming and earlier onset of snow melt [Warren, 1984; Jacobson, 2004; Hansen and Nazarenko, 2004; Flanner *et al.*, 2007] and a decrease in snowpack actinic flux, which will affect in-snow photochemistry [Honrath *et al.*, 2002; Grannas *et al.*, 2007 and references therein; Reay *et al.*, 2012]. Snow albedo can be reduced by a variety of impurities, such as light-absorbing carbon from combustion sources, mineral oxides in dust, soil organics, volcanic ash, algae, and other

biological organisms and constituents. The concentrations of these constituents in surface snow are determined by their mixing ratio in precipitation (wet deposition), the amount deposited to the surface via dry deposition, mechanical mixing of local soils and other organic matter with the existing snowpack, biological growth in the snow, and impurity redistribution in the snowpack via post-depositional processes such as wind-driven drifting, sublimation, and melt. Vapor loss from the snowpack to the atmosphere by sublimation in winter can cause enhanced concentrations of impurities at the top surface before the onset of snowmelt, as was seen in some Arctic profiles in Doherty *et al.* [2010].

[3] In this paper, we focus on the effects of snowpack melt on ILAP concentrations in surface snow. It has been hypothesized that, due to relatively inefficient incorporation of hydrophobic particulates into water, the mixing ratio of black carbon in snow meltwater is less than that in the melting snow, so a fraction of the BC from melted snow is added to that in the remaining surface snow. This process, which we call melt amplification, would amplify snow-albedo reduction and therefore provide a positive feedback to radiative forcing and climate warming by black carbon in snow [Flanner *et al.*, 2007, 2009]. Estimates of the magnitude of this effect to date are based largely on the work of Conway *et al.* [1996], who conducted experiments in which hydrophobic soot (“lamp-black,” from hydrocarbon

<sup>1</sup>Joint Institute for the Study of the Atmosphere and Ocean, University of Washington, Seattle, Washington, USA.

<sup>2</sup>Department of Atmospheric Sciences, University of Washington, Seattle, Washington, USA.

<sup>3</sup>Norwegian Polar Institute, Fram Centre, Tromsø, Norway.

<sup>4</sup>Atmospheric Sciences Research Center, University at Albany-State University of New York, Wilmington, New York, USA.

Corresponding author: S. J. Doherty, Joint Institute for the Study of the Atmosphere and Ocean, University of Washington, 3737 Brooklyn Ave. NE, Seattle, WA, 98105, USA. (sarahd@atmos.washington.edu)

combustion), hydrophilic soot (combustion products treated with a surfactant), and volcanic ash were each mixed in a bucket with ambient snow, then spread uniformly in a 2.5 cm deep layer over melting snow on a temperate glacier during summer. Surface albedo was monitored as the snow melted, and water loss (ablation by both melting and sublimation) was determined by monitoring snow depth on a network of stakes. Over the course of the experiment, approximately 125 cm of snow depth was lost to ablation. Profiles of soot and ash concentrations in the top 30 cm of the snow were measured at the end of the experiment period and compared to the initial concentrations in the top 2.5 cm.

[4] *Conway et al.* [1996] found that volcanic ash remained largely at the snow surface (top 15 cm), indicating that particles larger than 5 $\mu$ m are not efficiently washed down with melt. This is consistent with an earlier study looking at ~4–10  $\mu$ m diameter particulate (primarily dust/soil) in a “perennial snow patch” at 2700 m in the mountains of Japan, where it was found that the total particulate mass in the snow was the same after melt as before melt, implying zero scavenging with melt [*Higuchi and Nagoshi*, 1977].

[5] In contrast, *Conway et al.* found that after considerable melting the surface snow concentration of hydrophilic soot was less than 1% of its initial value in the top 2.5 cm but still present, but undetectable deeper in the snowpack. The surface snow concentration of the hydrophobic soot was about twice that of the hydrophilic soot, and hydrophobic soot was found in the snow throughout the measured 30 cm snowpack depth. The fact that the soot was initially present only in the top 2.5 cm of the snow yet some remained in the surface snow after more than a meter of snow was lost to ablation (primarily melt) indicates that even hydrophilic soot does not move through the snowpack with the same efficiency as meltwater. However, both hydrophobic and hydrophilic soot are scavenged more efficiently with meltwater than is volcanic ash, presumably because of their smaller size.

[6] The first global model study of snow BC radiative forcing to include amplification of surface snow BC concentrations with melt was presented by *Flanner et al.* [2007]. The model used by *Flanner et al.* includes hydrophobic and hydrophilic BC aerosol in the atmosphere. Both are deposited to snow, the former preferentially through dry deposition since it does not make an effective cloud condensation nucleus. *Flanner et al.* equated the synthetic soot used in the *Conway et al.* [1996] experiments to ambient BC in snow and used their study to estimate that 20% of hydrophilic and 3% of hydrophobic BC is scavenged with meltwater. They also ran sensitivity tests allowing the scavenging efficiency to range from 2% to 200% (hydrophilic BC) and 0.3–30% (hydrophobic BC), which produced global, annual average radiative forcings by BC in snow that were 69% and 108% of the central forcing estimate, respectively [see *Flanner et al.*, 2007, Table 4]. These estimated “BC scavenging ratios” of 20% and 3% were also used in the study of *Flanner et al.* [2009] and are available as the SNICAR model component of the Community Land Model (CLM) of the Community Earth System Model (CESM). The model studies of *Rypdal et al.* [2009] and *Skeie et al.* [2011] using the Oslo CTM2 model also include amplification of surface snow BC with melt by simply allowing all BC in the snow to remain at the snow surface (i.e., a 0% scavenging

efficiency), thereby giving the maximum possible amplification of radiative forcing.

[7] Other than the *Conway et al.* [1996] experiments, little data are available to determine the degree to which BC does in fact concentrate at the snow surface with melting. At one sampling site on the Tibetan Plateau, *Xu et al.* [2006] found that after 2 days of melting BC concentrations in surface snow increased by approximately a factor of 8 and particulate organic carbon (OC) by a factor of 2. The difference in BC versus OC mobility through the snowpack is presumably related to BC being more hydrophobic than OC and therefore less likely to be washed down through the snow with meltwater. *Xu et al.* [2009] extrapolated on this finding by assuming all BC remained in the snow with melt, distributing the BC evenly through the remaining snowpack, and reporting the expected change in snow BC concentration based on measured snow melt rates on a glacier in the southeast corner of the Tibetan plateau. *Aamaas et al.* [2011] noted that concentrations of BC in melting surface snow at several sites in Svalbard, Norway, were higher than in the cold snowpack earlier in the year and attributed some of the enhancement to melt amplification. *Doherty et al.* [2010] showed a greater than tenfold increase in snow BC concentrations in the melting layer of a snow pit near the Dye-2 station in the percolation zone of Greenland in 2008, and they attributed this to melt amplification. *Doherty et al.* also show elevated concentrations of light-absorbing particles and BC in melting surface snow in northeast Greenland (80°N, 26°W in August 2006; the KPCL site in Table 6 of *Doherty et al.*, [2010]). Earlier measurements near the Dye-3 site (also in Greenland, at higher elevation than Dye-2) in May similarly show concentrations in surface snow about a factor of 5 higher than in the sub-surface snow [*Clarke and Noone*, 1985]. (Note that *Clarke and Noone* [1985] erroneously refer to samples GR03 and GR05 in their text; in fact samples GR01 and GR03 are the near-surface snow samples and the other samples from deeper in the profile [Antony Clarke, personal communication]). However, *Doherty et al.* [2010] found that concentrations of BC in the summertime surface granular layer of melting sea ice were similar to those measured earlier in the springtime snow over sea ice, so there flushing of BC with melting appears to be effective. The difference here may be that while seasonal snow cover disappears completely, once the snow melts off the sea ice surface, flushing continues in the surface granular layer of sea ice throughout the summer. The surface granular layer occurs in well-drained melting sea ice; visually it resembles coarse-grained snow (corn snow) [e.g., *Perovich et al.*, 2002].

[8] In the springtime snowpack near Cherskiy (Russia) before melting had begun, *Doherty et al.* [2010] found that surface concentrations were a factor of 2 higher than sub-surface concentrations. They attributed this to a combination of sublimation, dry deposition, and possibly self-cleaning of the deep snow through depth hoar formation, since at that sampling site the snow falls mainly in autumn and the atmosphere is dry and windy in the winter and spring. This highlights the fact that measurements of elevated BC concentrations in surface snow do not necessarily point to melt amplification.

[9] Here we report on field measurements from three locations designed to quantify the enhancement of BC

concentration in surface snow with melting. Snow samples were gathered on first-year sea ice near Barrow (Alaska), on the southern part of the Greenland ice sheet, and on a mountain plateau above Tromsø (Norway) during each area’s melt season. A spectrophotometer using the integrating-sandwich principle [Grenfell *et al.*, 2011] was used to determine the concentrations of BC and other light-absorbing particulate constituents in the snowpack. The absorption Ångström exponent,  $\hat{a}_{\text{abs}}$ , the slope of light absorption versus wavelength in log/log space, is also measured by the spectrophotometer and provides an indication of whether the sources of light-absorbing particles differ at different layers in the snowpack, as well as whether the composition of the light-absorbing particulates in the snow changes with melt. Selected snow samples were also analyzed for several anions, providing further information on the sources of light-absorbing particulates and providing insight to the differential mobility of soluble versus non-soluble species through the snowpack with melt. Concentrations in the melting snow are compared to concentrations in deeper snow (Barrow, Tromsø, and Greenland) or in new snowfall (Greenland), resulting in amplification factors for surface snow ILAP due to melt amplification. Estimates of the fraction of light-absorbing particles scavenged with meltwater (i.e., analogous to the Flanner *et al.* [2007] scavenging efficiencies for BC) are given for the Barrow and Greenland 2010 field measurements. In Table 1, we give descriptions of the key acronyms and variables used in this paper.

## 2. Sampling Sites

### 2.1. Barrow, Alaska

[10] Snow samples were gathered on the sea ice in Elson Lagoon approximately 10 km to the east-northeast of Barrow at two sites, starting with a cold (unmelted) snow

**Table 1.** Definition of Key Acronyms and Variables Used in This Paper

BC	black carbon
ILAP	insoluble light-absorbing particulates
SWE	snow water equivalent
$\hat{a}_{\text{abs}}$	absorption Ångström exponent, calculated for 450–600 nm wavelengths
$L$	BC-equivalent mass concentration in snow ( $\text{ng g}^{-1}$ or ppb) of all insoluble light-absorbing particulates in snow, based on total light absorption measured in the 650–700 nm wavelength range
$B$	estimated BC concentration in snow ( $\text{ng g}^{-1}$ or ppb), made by assuming total absorption results from a linear combination of absorption by BC with $\hat{a}_{\text{abs,BC}}$ of 1.0 and non-BC constituents with $\hat{a}_{\text{abs,non-BC}}$ of 5.0
$S$	sulfate concentration in snow (ppm or ppb)
$A_L, A_B$	amplification factor describing the higher ILAP ( $L$ ) or BC ( $B$ ) concentration in surface snow relative to concentrations in sub-surface snow or in newly fallen snow
$A_L', A_B'$	for the Barrow data set only; $A_L$ and $A_B$ normalized to the sub-surface concentrations $L$ and $B$ in snow pre-melt, to account for pre-melt vertical variations in concentration not due to melt amplification
$m_L$	the average mass per unit volume of ILAP in the unmelted snow which melts by time $t$
$m_L'$	the average mass per unit volume of ILAP in the melting surface layer of snow at time $t$
$r_L, r_B$	the fraction of the ILAP ( $r_L$ ) or BC ( $r_B$ ) mass that remains in the snow surface layer with each increment of melt
$s_L, s_B$	the fraction of the ILAP ( $s_L$ ) or BC ( $s_B$ ) mass that is scavenged with meltwater, i.e., the melt “scavenging efficiencies” for ILAP and BC

pack on 21 May 2010 and ending on 11 June when about one third to one half of the initial snowpack depth remained. Compared with other areas in the region near and on the tundra and the active sea ice, the overall snow cover on the Lagoon was spatially very homogeneous but with local thickness variations due to sastrugi. Three sites separated by  $\sim 0.5$  km were initially surveyed to test for variability in BC loading. Sites 2 and 3 were located farther to the east and showed approximately the same loading while site 1 showed slightly higher levels. Site 2 was accordingly designated as the primary sampling location, but periodic sampling was also carried out at site 1. Snow thickness only was measured at site 3 on three occasions. The values showed a pattern consistent with that at the other two sites. Prevailing winds in the area are from the northeast; local winds were monitored during the measurement campaign for southwest winds that might transport emissions from the town of Barrow to the sampling site. Only one day of light SW wind occurred, but this did not appear to produce significant modification of the snow surface loading.

[11] Sample profiles were gathered throughout the snowpack depth at a typical vertical resolution of 2 cm. Two profiles were gathered on each sampling day at each site; results reported below are averages of these two side-by-side profiles to test for meter-scale horizontal variations, which were small in nearly all cases. Successive days’ pits were dug in a pattern moving upwind from southwest to northeast so that sampling activity on one day would not contaminate sampling sites of subsequent days.

[12] At each site, snow depth was recorded at ablation stakes located at the four corners of a  $\sim 50$  m  $\times$  50 m box which contained each site’s sample pits. Snow density was also recorded near each sampling site at  $\sim 3$  cm vertical resolution, in order to keep track of snowpack mass distribution. We used a Taylor-LaChapelle snow density kit, with a cutter of height 3 cm and volume  $100$  cm<sup>3</sup>. Some variation in snow depth was present in the boxes on a 1–10 m scale due to the presence of sastrugi. This is a common feature of natural snow cover in the area and has been included as an uncertainty in our analysis.

[13] All samples were gathered in Whirlpak bags and kept frozen until they could be rapidly melted and filtered in the lab at the UIC-NARL facility at Barrow using the procedures described by Doherty *et al.* [2010]. Selected meltwater samples were also saved and re-frozen for chemical analysis at the University of Washington.

### 2.2. Greenland

[14] The Dye-2 station on the Greenland ice sheet is located in the percolation zone at 2099 m altitude: in the summer the surface snow gets warm enough to melt, but the snow below the surface is cold enough that the meltwater re-freezes within the snowpack. Two sets of data from near Dye-2 are included in this analysis. On 24 July 2008, as part of a larger survey of Arctic snow ILAP, samples were gathered with  $\sim 2$ –5 cm vertical resolution from the surface down to 64 cm depth at  $65^\circ 57.12' \text{N}$ ,  $46^\circ 25.98' \text{W}$ ,  $\sim 60$  km south (climatologically upwind) of the Dye-2 station in the designated “research area,” as well as 30 km from the station. These pits showed higher BC concentrations in the near-surface layer, which had been affected by melting, lower concentrations in new snow on top of the melt layer,

and similarly low concentrations below the melt layer (Figure 1). This finding prompted our interest in returning to the Dye-2 station to conduct further measurements of BC in melting snow.

[15] In summer 2010, we returned to Dye-2 and gathered snow at two sites ( $66^{\circ}12.95'N$ ,  $46^{\circ}10.54'W$  on 21 and 23 July and  $66^{\circ}12.70'N$ ,  $46^{\circ}22.69'W$  on 24 July), also in the “research area”  $\sim 30$  km south of the station. At the first site, snow was sampled at typically 2 cm vertical resolution from the surface down to 206 cm. At the second, snow was sampled at 1 cm resolution from the surface down to 20 cm, then at 2 cm resolution from 20 cm to 100 cm depth. At both sites, samples were gathered in two parallel pits about 50 cm apart. This produced a large number of samples ( $>600$ ), so we analyzed the full set of samples from only one of the pits at each site, then analyzed a subset of the samples from the second pit (bracketing the depths at which BC was changing rapidly in the first pit). Snow density was also measured at 4 cm vertical resolution in a pit parallel to the snow sampling pits. The density in the top 60 cm averaged  $415 \text{ kg m}^{-3}$ ; below 60 cm it averaged  $\sim 490 \text{ kg m}^{-3}$  not including the ice lenses, of which there were many below  $\sim 120$  cm (pit 1). Samples of newly fallen snow had been gathered earlier at the Dye-2 station (Raven Camp) by the station staff between 1 May and 1 July 2010, and these are used to establish baseline concentrations of BC in snow not yet affected by in-snow processes such as melt, sublimation, and mechanical mixing with wind.

### 2.3. Tromsø, Norway

[16] Snow was collected in May 2008 on a mountain plateau (Fjellheisen) at elevation 420 m above and to the

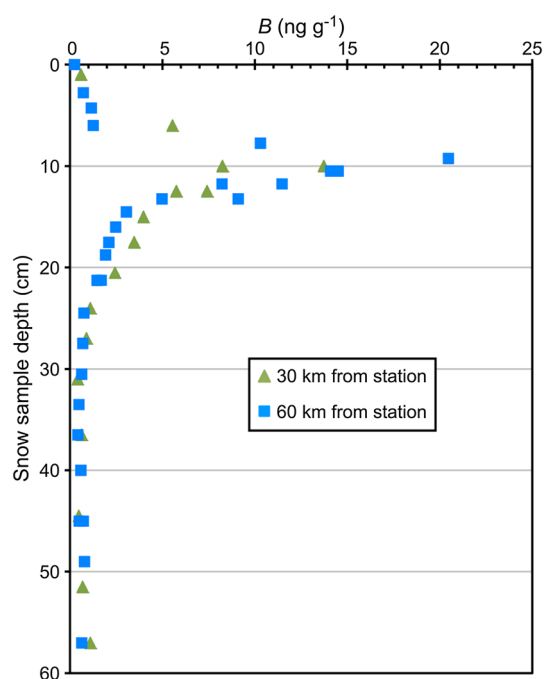


**Figure 1.** The estimated concentration of BC,  $B$ , in snow samples gathered in July, 2008 from two sites upwind from the Dye-2 research station on the Greenland ice sheet. This profile included a melt layer, buried by a few centimeters of newly fallen snow (modified from Figure 10a of *Doherty et al.* [2010]).

east of the city of Tromsø, Norway ( $\sim 69.5^{\circ}N$ ,  $19.0^{\circ}E$ ) immediately preceding the onset of melt (19 and 21 May), then on 21, 23, 26, 28, and 30 May, when the snowpack was in the process of melting, with rain events on 27 and 28 May. These data were mentioned in the Arctic survey of *Doherty et al.* [2010] and are discussed in detail herein. On all of these days, snow was collected throughout the snowpack depth, typically at 3 cm vertical resolution for the top 12 cm of the snowpack, then with 5–10 cm resolution below that, with total snow depths of 17–30 cm.

[17] Vertically resolved snow samples were also gathered at the same site in 2010, but in this case the sampling started after melting had commenced so in all cases the snow BC concentration had been affected by melt redistribution.

### 3. Sample Analysis

[18] Snow sample analysis follows directly that described by *Doherty et al.* [2010]. Briefly, snow samples are spooned into a glass beaker and rapidly melted in a microwave oven, then drawn via vacuum through a  $0.4 \mu\text{m}$  nucleopore filter. Filters are dried, then analyzed with the laboratory spectrophotometer for spectrally resolved (400–750 nm at 10 nm resolution) light absorption by insoluble particles. Measured absorption is converted to an equivalent BC mass loading on the filter using a set of calibration standard filters loaded with pure synthetic black carbon which has a mass absorption efficiency (MAE) of  $\sim 6 \text{ m}^2 \text{ g}^{-1}$  at 550 nm; thus, derived masses are an “equivalent mass” for BC with that MAE. If the sample BC MAE is in fact higher, such as suggested by *Bond and Bergstrom* [2006], the true mass of BC is lower; however, absorption of radiation in the snow is correctly represented by the concentrations we present if an MAE of  $6 \text{ m}^2 \text{ g}^{-1}$  is used. Mass loadings on the filters are converted to mass mixing ratios ( $\text{ng g}^{-1}$ ) in the snow based on the filter’s exposed area and the volume of snow meltwater drawn through the filter.

[19] Samples from Barrow and Dye-2 were collected in Whirlpak bags and experienced some melt in the bags before being spooned into a glass beaker for melting in the lab. As discussed by *Wang et al.* [2013], we later discovered that a surfactant in the bags would scavenge some of the particulates in the melted snow water and these would be left behind in the beaker as a “scum ring.” An empirical correction factor that is a function of ILAP concentration is used here to correct for these losses [see equation (1) of *Wang et al.*, 2013]. A 15% correction for undercatch by the  $0.4 \mu\text{m}$  nucleopore filters was also applied based on catch efficiency tests, as reported by *Doherty et al.* [2010].

[20] A maximum possible BC concentration with units of ppb or  $\text{ng g}^{-1}$  is derived by attributing all absorption in the 650–700 nm wavelength range to BC. This concentration, which we will call  $L$ , accounts for absorption by all ILAP, quantified as an equivalent black carbon concentration needed to account for all 650–700 nm particulate absorption. Snow albedo is affected by all light-absorbing particulates, not just black carbon, so we focus below on how profiles of  $L$  in snow vary with melt.

[21] A metric for variations in the spectral absorption characteristics (color) of the total particulate in the snow is given by the absorption Ångström exponent,  $a_{\text{abs}}$ , defined as

$$\hat{a}_{abs} = -\ln\left(\frac{\sigma_{\lambda_1}}{\sigma_{\lambda_2}}\right) \bigg/ \ln\left(\frac{\lambda_1}{\lambda_2}\right) \quad (1)$$

where  $\sigma_{\lambda_1}$  and  $\sigma_{\lambda_2}$  are the light absorption coefficients (or light absorption optical depths) at wavelengths  $\lambda_1$  and  $\lambda_2$ . Herein, values of  $\hat{a}_{abs}$  are for  $\lambda_1 = 450$  nm and  $\lambda_2 = 600$  nm.

[22] An estimate of the BC concentration,  $B$ , is made by assuming total absorption results from a linear combination of absorption by BC with  $\hat{a}_{abs,BC}$  of 1.0 and non-BC constituents with  $\hat{a}_{abs,non-BC}$  of 5.0 [Doherty *et al.*, 2010; Kirchstetter *et al.*, 2004; Roden *et al.*, 2006; Sun *et al.*, 2007]. Uncertainty in this apportionment becomes large when  $\hat{a}_{abs}$  becomes large (e.g., uncertainty  $>50\%$  for  $\hat{a}_{abs} > 2.8$ ; see Figure 16 of Doherty *et al.* [2010], noting that therein  $B$  is referred to as  $C_{BC}^{est}$ ).

[23] Here we are interested in the redistribution of all light-absorbing particulates at the snow surface with melt, so we focus on how vertically resolved  $L$  in the snow evolves with melt, and we use  $\hat{a}_{abs}$  as a metric for whether the relative contributions to total absorption by BC and non-BC constituents changes with melt. Smaller and/or more soluble particles should be scavenged more efficiently with meltwater than larger or less soluble particles. Therefore the relative scavenging rates of BC versus non-BC absorbers will vary with their size and composition. If meltwater scavenging rates of BC are lower than for other ILAP constituents,  $\hat{a}_{abs}$  will decrease with melt; if the rates are lower,  $\hat{a}_{abs}$  will increase. Therefore  $\hat{a}_{abs}$  is also presented for both the cold and melting snowpack samples.

[24] In addition to this optical analysis, a subset of the snow samples was analyzed chemically for soluble constituents (formate, chloride, nitrate, succinate, sulfate, and oxalate) using ion chromatography. We expect that ions will be washed down through the snowpack with about the same efficiency as the snow meltwater, so we examine the differential change in the vertical distribution of absorbing particulate matter ( $L$ ) versus that of the ions.

#### 4. Results for Barrow, Alaska

[25] Sampling started on 21 May 2010 with a cold snowpack with an upper layer of windpack over a layer of lower density ( $<300$  kg/m<sup>3</sup>) depth hoar that was about 14 cm thick at site 2 on 24 May (Figure 2b) and had metamorphosed by 1–3 June into a compacted high density layer (about 400 kg/m<sup>3</sup>). Freezing rain fell on 23 and 28 May, then on 31 May to 1 June,  $\sim 4$ –5 cm of new snow fell in windy conditions. By 24 May, a layer of “superimposed ice” (SPI) had formed at the bottom of the snow on the surface of the sea ice, as shown for site 2 in Figure 2b. Superimposed ice is formed when meltwater from near-surface snow percolates down through the snowpack then refreezes in the bottom of the snowpack, where temperatures are still below freezing. At all three mass balance sites, superimposed ice was present and remained intact until at least 11 June. The SPI densities of 850 kg/m<sup>3</sup> presented in Figure 2 are an estimate based on previous experience with desalinated multiyear sea ice core samples [e.g., Grenfell, 1992] compared with the observed texture and hardness of the superposed ice. By the end of the experiment, the superimposed ice had begun to decay. After 1 June, there was no rain or new snow and the snowpack rapidly melted, with the total depth decreasing from 30–35 cm on 1 June to approximately 10–15 cm on 11 June (Figure 3). As the snowpack melted, the depth hoar crystals underwent destructive metamorphism and the layer densified and compacted.

[26] Between 24 and 30 May, the snow water equivalent (SWE) was roughly constant at  $\sim 7$  g cm<sup>-2</sup>. The new snowfall on 30–31 May increased total snowpack SWE to about 9–10 g cm<sup>-2</sup>, where it remained until about 9 June. Thereafter the snowpack mass began to decay because the entire snowpack had risen to the melting temperature; SWE dropped to  $\sim 5$ –6 g cm<sup>-2</sup> by 11 June. Based on the rapidity of snow loss and the ambient temperature and winds during the sampling period, it is clear that the snow loss was dominated by melt, not sublimation, although it is not possible to quantify their relative contributions.

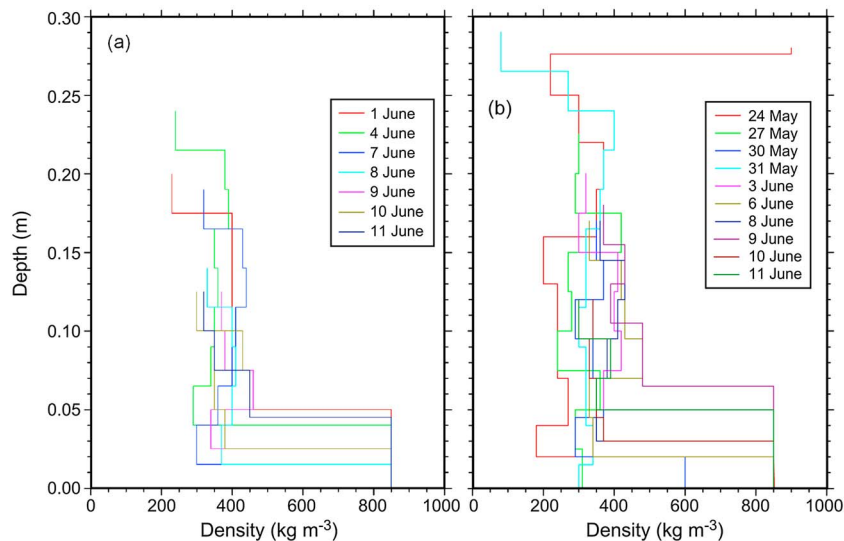


**Figure 2.** Profiles of snow density at (a) site 1 (71°19.51'N, 156°25.99'W) and (b) site 2 (71°19.50'N, 156° 24.26'W) near Barrow, Alaska, over the period of our measurements. The density of 850 kg/m<sup>3</sup> for the superimposed ice is an estimate as described in the text.

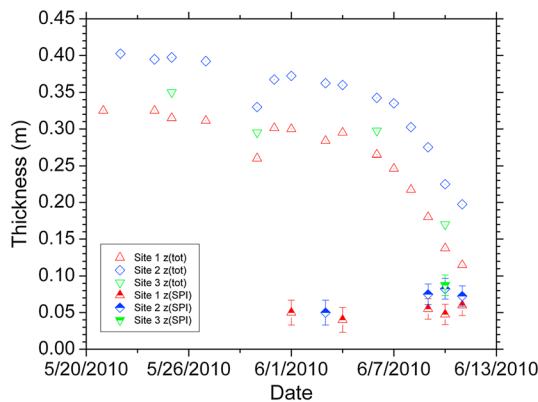


**Figure 3.** The evolution of snow thickness at the Barrow sampling sites. SPI is the superimposed ice layer that appeared at the bottom of the snowpack on top of the sea ice, which can be seen as a layer of high density in Figure 2.

[27] Each ILAP profile was taken at a slightly different location (up to a few meters apart) within each  $50\text{ m} \times 50\text{ m}$  region defining the two sites. Snow depth across the sites typically varied by  $\sim 10\text{--}15\%$ . With aging, compaction reduced the snow depth without any loss of water content. Thus, total measured snow depth varies from one profile to the next even in the absence of new snowfall or ablation. This is apparent, for example, in the lower snowpack depths on 1 June relative to 21 May at Site 1 (Figure 3), despite there being 4–5 cm of new snow on 1 June. This is likely a combination of compaction of the snow between 22 May and 1 June and natural variations in total snowpack depth at the two sampling locations.

#### 4.1. ILAP Profiles

[28] The Barrow profiles (Figure 4) tell a mostly consistent story. However, the sample profile from 3 June at site 2 is anomalous, with both much higher values of  $L$  (Figure 4c)

and much lower values of  $\hat{a}_{\text{abs}}$  (Figure 4d). This entire profile appears to have been contaminated somehow, although we cannot explain how this one location within the  $50\text{ m} \times 50\text{ m}$  site could have been so systematically affected throughout the snowfall season. It is possible that all of these samples were somehow contaminated during collection or processing, but this seems unlikely given the care taken during sampling and analysis. In any case, because this is a clear outlier we exclude this profile from our discussion and subsequent analysis of the evolving snowpack.

[29] Several things are apparent from the Barrow profiles. Before melting started,  $L$  was about  $5\text{--}15\text{ ng g}^{-1}$  in the bottom half of the snowpack and about  $10\text{--}30\text{ ng g}^{-1}$  in the upper half of the snowpack, with a few samples as high as  $30\text{--}45\text{ ng g}^{-1}$  (Figures 4a and 4c). There is no systematic variation with depth for  $\hat{a}_{\text{abs}}$  except in the top approximately 10 cm, where it steadily decreases toward

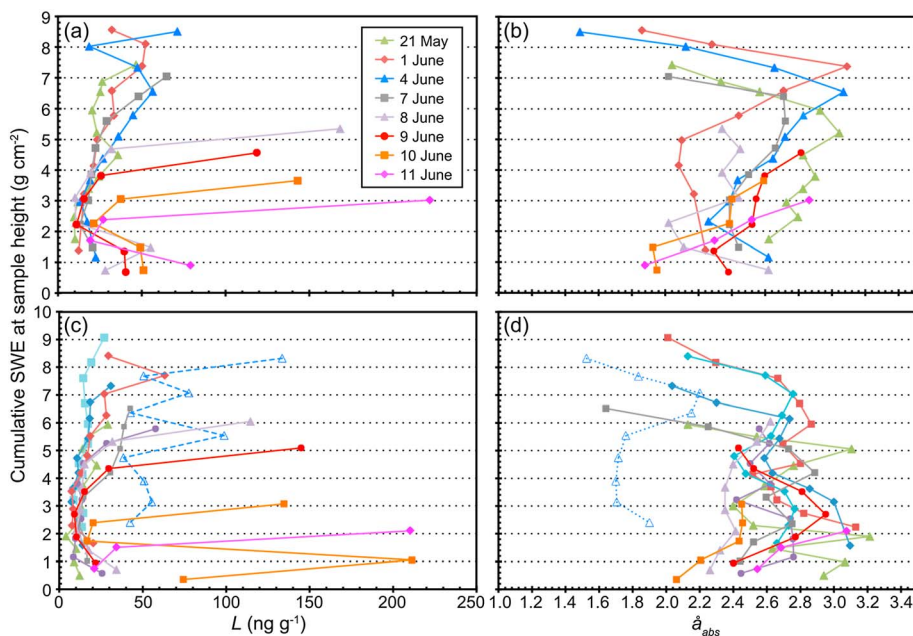


**Figure 4.** Profiles near Barrow, Alaska, in 2010 of  $L$  at (a) site 1 and (c) site 2, and of  $\hat{a}_{\text{abs}}$  at (b) site 1 and (d) site 2. Data are shown as a function of the cumulative snow water equivalent (SWE) from the sea ice surface up to the snow sample. Meltwater incorporated into superimposed ice is not included in the calculating of SWE.

the top (Figures 4b and 4d). Lower values of  $\hat{a}_{\text{abs}}$  are consistent with a shift away from a biomass burning source toward a fossil fuel source [Millikan, 1961; Rosen *et al.*, 1978; Kirchstetter *et al.*, 2004; Bergstrom *et al.*, 2007; Clarke *et al.*, 2007], although other explanations are also possible. If we assume most particulate snow impurities result from wet deposition as is given by many global modeling studies [e.g., Flanner *et al.*, 2007, 2009; Jacobson, 2004; Koch *et al.*, 2009], the increase in concentrations toward the surface indicates that the mixing ratio of ILAP to snow mass is higher in late spring than earlier in the accumulation season. Alternatively, this could result from an increase in dry deposition of aerosols to the snow surface. In either case, lower values of  $\hat{a}_{\text{abs}}$  near the surface indicate that the source of impurities shifted in late spring/early summer, although this is not associated with a notable shift in total source intensity.

[30] As the snow melted the concentrations in the melting surface snow increased, eventually exceeding  $200 \text{ ng g}^{-1}$  (Figures 4a and 4c). The subsurface snow concentrations initially were unaffected, but later in the melt season  $L$  deeper in the snowpack (i.e., in the bottom-most samples) also increased. This was likely due to the wash down of snow meltwater from the surface snow which—even though it contained only a fraction of the surface snow particulate concentration—brought higher concentrations of BC and other light-absorbing particulates downward in the snowpack, which by then was saturated with meltwater [Xu *et al.*, 2012].

#### 4.2. Mobility of Different ILAP Through the Snowpack

[31] The composition of the surface snow particulates also appears to change with melt, with  $\hat{a}_{\text{abs}}$  in the surface snow increasing from 4 June to 11 June, especially at site 1 (Figure 4b). This might result from smaller, BC-containing

(e.g., combustion) particles being washed through the snowpack with higher efficiency than larger particles, such as soil or mineral dust, which have a higher absorption Ångström exponent. In contrast to the particulate impurities, most of the snowpack chloride, nitrate and sulfate appear to have been removed from the snowpack with melt as expected, but the concentration of succinate is relatively unaffected by melt (Figure 5).

#### 4.3. Vertical Redistribution and Solubility

[32] Recent studies have shown that both chloride and nitrate concentrations in snow can be affected by in-snow photochemistry [e.g., Grannas *et al.*, 2007]. Indeed, BC and nitrate may even be photochemically linked [Reay *et al.*, 2012]. Succinate is only partially soluble and so might not be as efficiently washed down through the snowpack with meltwater, as appears to be the case (Figure 5). Sulfate, however, is soluble and also will be largely unaffected by in-snow photochemistry. The ratio of  $L$  to sulfate concentration ( $S$ ) therefore reflects the difference in their solubility and wash-down with melt (Figure 6). Focusing on site 2, where we have several profiles for both  $L$  and sulfate concentrations, we see that before the onset of melt (22 May)  $L/S$  peaked immediately below the snow surface then declined with depth. On 31 May there had been some melting and the ratio  $L/S$  increased by a factor of about 8–9 relative to samples from the same depth on 22 May at site 2. As melt progressed (9 and 10 June),  $L/S$  continued to increase throughout the snowpack, with sulfate concentrations low enough to be below our measurement threshold for many of the later samples. This is consistent with the preferential retention of ILAP at the snow surface and preferential wash down of sulfate with melt.

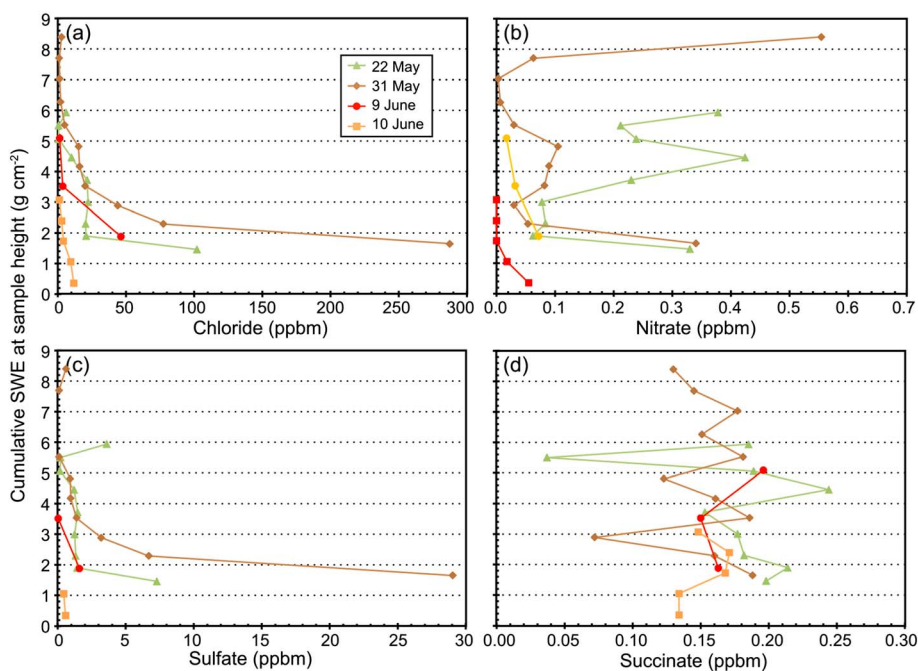


**Figure 5.** Concentrations of (a) chloride, (b) nitrate, (c) sulfate, and (d) succinate in the snow at Barrow site 2, on 2 days before any significant melting had occurred (22 and 31 May) and after more than half the snowpack had melted (9 and 10 June).

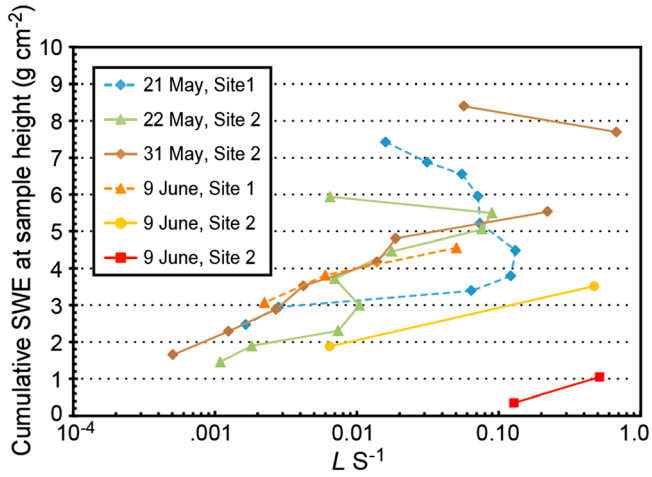


**Figure 6.** Ratio of BC concentration to sulfate concentration at Barrow, versus height in the snow.

#### 4.4. Amplification Factors for ILAP and BC

[33] Amplification factors for  $L$  ( $A_L$ ) and  $B$  ( $A_B$ ) are calculated as the ratio of the surface-to-subsurface sample averages, where the “surface” samples are from either the top 2 cm of the snowpack or the top 4 cm of the snowpack and the “subsurface” samples are those from 4 cm above the sea ice to 4 cm below the snow surface. The subsurface was defined this way because the lowermost sample might have included particles that were originally sitting on the sea ice below the snowpack but became mixed in with the lowest sample layer once it was saturated with meltwater.

[34] If  $L$  and  $B$  were constant through the snowpack depth before melt,  $A_L$  and  $A_B$  would be 1. In fact on 31 May to 1 June, immediately before melt commenced, ILAP and BC concentrations were higher at the surface than in the subsurface in the unmelted snow (Table 2). Therefore, some of the enhancement ( $A_L$  and  $A_B > 1$ ) seen later in the melting snow is due to initially higher concentrations in the surface snow than in the subsurface snow. To estimate the effect of melt only, we normalize the amplification factors by their average values from 21 to 22 May to get the scaled quantities  $A_L'$  and  $A_B'$  (Table 2).

[35] It is apparent that the amplification in particulate concentrations is almost completely confined to the top 2 cm of the snowpack (Figure 4). However, the e-folding depth for mid-visible sunlight in snow is typically 3–10 cm or deeper [e.g., France *et al.*, 2011; Reay *et al.*, 2012] so amplification factors for just the top 2 cm of the snowpack exaggerate the effect on snow albedo. The depth of snow in the topmost layer in model studies is typically ~2–5 cm; for models with a surface layer at the higher end of this range, the amplification factors for the top 4 cm of the snowpack are the more appropriate comparison.

[36] Both  $A_L'$  and  $A_B'$  showed a small increase between 21 and 27 May as the snowpack warmed and started to melt and there were two episodes of freezing rain. On 30 May, there was a larger increase in the amplification factors, but on 31 May and 1 June new snowfall produced a decline in surface snow concentrations and therefore in both  $A_L'$  and  $A_B'$ , to values lower than in even the cold (pre-melt) snowpack of 21–22 May. Moderate amounts of melt on 1–6 June produced only small changes in snow depth (Figures 3 and 4)

**Table 2.** Amplification Factors for the Concentration of Light-Absorbing Particles in Surface Snow on Sea Ice Near Barrow, Alaska During the 2010 Melt Season<sup>a</sup>

Sampling date (site #)	(a) Surface to Subsurface Amplification Factors				(b) Amplification Factors, Normalized to 21–22 May Average			
	Top 2 cm		Top 4 cm		Top 2 cm		Top 4 cm	
	$A_L$	$A_B$	$A_L$	$A_B$	$A_L'$	$A_B'$	$A_L'$	$A_B'$
21 May (1)	2.1	2.6	1.6	2.0	1.2	1.2	1.1	1.1
22 May (3)	1.5	1.7	1.4	1.6	0.8	0.8	0.9	0.9
22 May (2)	2.3	2.7	1.9	2.1	1.3	1.3	1.2	1.2
24 May (2)	2.0	2.4	1.6	1.8	1.1	1.1	1.1	1.0
27 May (2)	2.5	3.0	2.0	2.4	1.4	1.4	1.3	1.3
30 May (2)	4.9	5.2	3.2	3.3	2.7	2.4	2.1	1.9
31 May (2)	1.3	1.5	1.3	1.5	0.7	0.7	0.9	0.8
1 June (1)	1.0	1.2	1.3	1.5	0.6	0.6	0.9	0.8
4 June (1)	2.2	2.9	1.4	1.8	1.2	1.3	0.9	1.0
6 June (2)	1.8	2.4	1.8	2.1	1.0	1.1	1.2	1.2
7 June (1)	2.9	3.3	2.5	2.7	1.6	1.5	1.7	1.5
8 June (1)	12.6	12.8	7.5	7.5	7.1	5.9	5.0	4.2
8 June (2)	8.9	8.6	5.7	5.5	5.0	4.0	3.8	3.1
9 June (1)	9.0	8.5	5.5	5.2	5.0	3.9	3.6	2.9
9 June (2)	12.0	14.1	7.2	8.5	6.7	6.5	4.8	4.8
10 June (1)	6.7	6.5	4.2	4.2	3.8	3.0	2.8	2.3
10 June (2)	8.1	8.1	4.6	4.7	4.5	3.8	3.1	2.6
11 June (1)	11.5	10.3	6.5	5.8	6.5	4.7	4.3	3.3
11 June (2)	10.0	8.8	10.0	8.8	5.6	4.1	6.6	5.0

<sup>a</sup>Calculated as (a) the ratio of the  $L$  or  $B$  in the top 2 or 4 cm of the snowpack to that in the sub-surface snow (4 cm deep to 4 cm above the sea ice) gives, respectively,  $A_L$  and  $A_B$ . (b)  $A_L'$  and  $A_B'$  have been normalized by the value of  $A_L$  and  $A_B$  in the cold snow samples on 21–22 May to separate the effect of melting, rather than seasonal changes in deposition, on surface snow ILAP and BC concentrations.

and correspondingly moderate increases in  $A_L'$  and  $A_B'$ . However, during 7–11 June, there was considerable melting, with total snow depth declining rapidly (Figures 3 and 4).  $A_L'$  and  $A_B'$  increased markedly starting on 8 June and remained high through 11 June, when most of the snowpack had melted. Note that neither the amplification factors (Table 2) nor the surface snow concentrations (Figure 4) showed a clear increase after 8 June; instead, they appear to have jumped rapidly by 8 June, then were high but variable thereafter.

[37] If BC in the particles is preferentially retained at the snow surface in comparison to non-BC absorbers,  $A_B'$  should increase more rapidly than  $A_L'$  as the snow melts. However this was not the case; instead,  $A_B'$  and  $A_L'$  were equal but as melt commenced  $A_B'$  became ~10–20% smaller than  $A_L'$ . Thus, it appears that the BC is more efficiently scavenged with meltwater than are the non-BC light-absorbers, though not dramatically so.

#### 4.5. ILAP and BC Scavenging Efficiencies

[38] Using the coincident measurements of snow density and  $L$ , it is possible to estimate the efficiency with which ILAP is scavenged with snow meltwater. This allows comparison to the values used in the Flanner *et al.* [2007; 2009] model studies.

[39] To calculate scavenging efficiencies we assume that as the surface snow melts each increment of meltwater leaves behind a certain fraction of its ILAP in the melting surface layer. We assume that when the next increment of water melts from the surface, the fraction of ILAP left

behind is the same; as a consequence the mass of ILAP left behind is higher than with the previous increment because the surface concentration is higher. This is perhaps the simplest representation of the melt-amplification process. The retention of BC in reality must depend on some variable properties of the snowpack, particularly the specific surface area and the thickness of the water films in wet snow. However, the limited data from our measurements cannot support a more comprehensive model than the simple treatment we use here.

[40] If we assume ILAP concentrations and snow density are vertically homogeneous in the snowpack before melt, and that the scavenging efficiency is a constant, the accumulation of ILAP in the melting surface layer is given by

$$m_L' = m_L(1 + r_L + r_L^2 + r_L^3 + r_L^4 + \dots + r_L^n) \quad (2)$$

where  $m_L$  is the average original mass per volume in the portion of the unmelted snowpack which has melted by time  $t$ ;  $m_L'$  is the average mass per unit volume in the melting surface layer of snow at time  $t$ ; and  $n$  is the number of increments of melt (i.e., SWE) within time  $t$ . The value  $r_L$  is the fraction of the ILAP mass that remains in the snow surface layer with each increment,  $n$ . As long as  $r_L$  is less than unity equation (2) is asymptotic, with convergence reached in fewer steps (smaller  $n$ ) for smaller values of  $r_L$ , so that

$$\frac{m_L'}{m_L} \approx \frac{1}{(1 - r_L)}. \quad (3)$$

[41] Using the measured values of  $m_L$  and  $m_L'$ , equation (3) can be used to determine  $r_L$ . The fraction of  $m_L$  that is scavenged with the meltwater is therefore given by

$$s_L = 1 - r_L. \quad (4)$$

[42] The values  $m_L$  and  $m_L'$  are calculated directly from the corresponding values of  $L$  and snow density. Equations (2)–(4) apply also to BC, using the corresponding values of  $B$  to calculate  $m_B$ ,  $m_B'$ ,  $r_B$ , and  $s_B$ .

[43] Our determination of  $r$  from equation (3) assumes that  $m'$  is measured after a sufficient amount of melt that  $m'$  has converged to its maximum value. If this is not the case, our inferred values of  $r$  will be too low and the scavenging efficiency,  $s$ , too large. Therefore, the values of  $s_L$  and  $s_B$  given here may represent upper limits.

[44] Our estimated BC concentrations,  $B$ , are more uncertain than our measure of  $L$  because they are calculated by apportioning light absorption to BC and non-BC constituents using assumed values of  $\hat{a}_{\text{abs}}$  for these two components. Thus,  $s_B$  is more uncertain than  $s_L$ . However, significant differences between the two indicate whether BC is scavenged more or less efficiently than the non-BC light-absorbing snow particulates (e.g., brown carbon, soil, and/or mineral dust) and therefore the relative roles of BC and non-BC absorbers in lowering snow albedo during the melt season. For example, if BC is scavenged with much higher efficiency than is soil or mineral dust (as concluded by Conway *et al.* [1996]), then in areas with significant snow soil or dust loading (e.g., north central China

[Wang *et al.*, 2013] more efficient scavenging of BC with melt may lead to non-BC absorbers dominating visible wavelength snowpack light absorption in spring.

[45] Equation (2) is accurate if the particulate impurity mass per unit volume (or, equivalently,  $L$  or  $B$ ) is uniform throughout the column of unmelted snow which eventually melts by time  $t$  and if it is uniform in the melting surface layer at time  $t$ . Since these conditions are not met we calculate  $s_L$  and  $s_B$  for a range of values of  $m_L$  and  $m_B$ . Concentrations in the melting surface layer after considerable melt are also variable and uncertain so we similarly calculate  $s_L$  and  $s_B$  for a range of values of  $m_L'$  and  $m_B'$ .

[46] At Barrow, approximately 16 cm of snow depth was lost at the sampling sites between 31 May and 11 June. Thus, we use the average concentrations  $L$  and  $B$  and the average snow densities in the top 16–17 cm of the snowpacks on 1 June (site 1) and 31 May (site 2) to get the average mass per unit volume,  $m_L$  and  $m_B$ , for the snow that eventually melts. These correspond to concentrations for  $L$  of  $35 \pm 12 \text{ ng g}^{-1}$  and  $26 \pm 17 \text{ ng g}^{-1}$ , respectively, and for  $B$  of  $26 \pm 8 \text{ ng g}^{-1}$  and  $19 \pm 13 \text{ ng g}^{-1}$ , respectively. We consider the best estimate of  $s_L$  to correspond to values of  $m_L$  using  $L = 25\text{--}35 \text{ ng g}^{-1}$ , but we also do calculations assuming  $L$  in this layer is as low as  $15 \text{ ng g}^{-1}$  and as high as  $45 \text{ ng g}^{-1}$ . We consider the best estimate of  $s_B$  to correspond to values of  $m_B$  using  $B = 20\text{--}25 \text{ ng g}^{-1}$ , but do calculations for  $B$  of  $10\text{--}35 \text{ ng g}^{-1}$ . The average snow densities in this layer were  $360 \pm 80 \text{ kg m}^{-3}$  and  $320 \pm 70 \text{ kg m}^{-3}$  at sites 1 and 2, respectively, so a value of  $340 \text{ kg m}^{-3}$  is used to convert  $L$  and  $B$  to  $m_L$  and  $m_B$ . (Note that variations in the assumed snow density of the unmelted snow of  $\pm 50 \text{ kg m}^{-3}$  result in changes in  $s$  of  $<1\%$  for values of  $s$  of  $5\text{--}10\%$  and a change of  $\sim 5\%$  for  $s = 40\%$ .)

[47] The masses  $m_L'$  and  $m_B'$  are calculated based on  $L$ ,  $B$ , and snow density from the surface sample, corresponding to the top 2 cm of the snowpack, at the end of our measurements. On 11 June,  $L$  and  $B$  in this layer were  $222 \text{ ng g}^{-1}$  and  $153 \text{ ng g}^{-1}$ , respectively, at Site 1 and  $210 \text{ ng g}^{-1}$  and  $135 \text{ ng g}^{-1}$  respectively at site 2. Therefore  $m_L'$  is calculated for  $L$  of  $160\text{--}260 \text{ ng g}^{-1}$ , with the values corresponding to  $200\text{--}220 \text{ ng g}^{-1}$  considered the “best estimate;”  $m_B'$  is calculated for  $B$  of  $115\text{--}175 \text{ ng g}^{-1}$ , with the values corresponding to  $135\text{--}155 \text{ ng g}^{-1}$  considered the “best estimate.” The snow densities in the top 2 cm layer at Sites 1 and 2 were, respectively,  $300$  and  $320 \text{ kg m}^{-3}$ , so we use a density of  $310 \text{ kg m}^{-3}$  to convert  $L$  to  $m_L$ .

[48] The scavenging efficiency of ILAP with snow meltwater,  $s_L$ , ranges from approximately 5% to 30% (Table 3) depending on the values of  $L$  used for the pre-melt and post-melt snow, with a best estimate range of  $\sim 10\text{--}20\%$ . As noted above our derived values of  $s$  may represent an upper limit. The fraction of BC scavenged with melt,  $s_B$ , is a few percent higher. Given the uncertainty associated with estimating BC concentrations from our measurements, we cannot assert that the values of  $s_L$  and  $s_B$  are significantly different. In this regard it is important to note that moderate change in  $s$  can produce a significant change in surface amplification; e.g., a change in  $s$  from 15% to 20% results in a change in the amplification factor from 7.3 to 5.3. Thus, the small apparent difference between  $s_L$  and  $s_B$  (Table 3) corresponds to a larger difference between the amplification factors for ILAP and BC ( $A_L'$  and  $A_B'$  in Table 2). This

**Table 3.** Scavenging Efficiencies for Barrow<sup>a</sup>

(a) $s_L$		$L$ Unmelted Snow ( $\text{ng g}^{-1}$ ):						
$L$ , Melted Snow ( $\text{ng g}^{-1}$ ):	15	20	25	30	35	40	45	
160	10%	14%	17%	20%	24%	28%	31%	
180	9%	12%	15%	18%	21%	24%	28%	
200	8%	11%	<b>14%</b>	<b>16%</b>	<b>19%</b>	22%	24%	
220	8%	10%	<b>12%</b>	<b>15%</b>	<b>17%</b>	20%	22%	
240	7%	9%	11%	13%	16%	18%	20%	
260	6%	9%	11%	12%	15%	17%	19%	
(b) $s_B$		$B$ Unmelted Snow ( $\text{ng g}^{-1}$ ):						
$B$ , Melted Snow ( $\text{ng g}^{-1}$ ):	10	15	20	25	30	35		
115	10%	14%	19%	24%	29%	33%		
125	9%	13%	17%	22%	26%	30%		
135	8%	12%	<b>16%</b>	<b>20%</b>	24%	28%		
145	8%	11%	<b>15%</b>	<b>19%</b>	23%	26%		
155	7%	11%	<b>14%</b>	<b>17%</b>	21%	25%		
165	7%	10%	13%	16%	20%	23%		
175	6%	10%	12%	15%	19%	22%		

<sup>a</sup>(a)  $s_L$  and (b)  $s_B$  corresponding to the concentrations  $L$  and  $B$  in the Barrow snow before it melted and in the surface layer affected by melt (here, the top 2 cm of the snowpack; Figure 1) after extensive melting. Calculations are based on equations (2)–(4), with “best estimate” values shown in bold.

points out the need for a better constrained measure of the scavenging efficiency of BC versus non-BC ILAP.

[49] The model we have presented for calculating  $s_L$  and  $s_B$  is based on the assumption that scavenging efficiencies are constant throughout the melting process. In fact scavenging efficiencies may vary with the rate of melt, evolving snow morphology, and other factors. As a first-order test of the sensitivity of our derived values of  $s_L$  and  $s_B$  to variations in scavenging efficiency through the melt process, we calculated how final concentrations ( $m_L'$  and  $m_B'$ ) would change if scavenging rates across the melt period are initially higher than their central value by 5% then lower by 5%, i.e., if  $s_L$  is 10%, we allowed it to be 5% then 15%. We then compared the resulting values of  $s_L$  and  $s_B$ ; this yields with the values of  $s_L$  and  $s_B$  inferred from our model assuming a constant scavenging rate. If scavenging efficiency varies in this manner, our derived values of  $s_L$  and  $s_B$  will be biased high by  $\sim 5\%$ . Conversely, if the scavenging efficiency is initially lower by 5% then higher by 5%, our estimates of  $s_L$  and  $s_B$  will be biased low by  $\sim 5\%$ . While this simple test does not cover the complexity of variations that may be occurring in ambient snowpacks, it does bound the uncertainties in  $s_L$  and  $s_B$  that result from moderate time variations in scavenging through the melt period. This uncertainty ( $\sim 5\%$ ) is independent of but comparable to the uncertainty due to imperfect constraints on the initial and final concentrations in snow, i.e., the range of values given in Table 3.

[50] These measured values of  $s_L$  and  $s_B$  are broadly consistent with the *Flanner et al.* [2007] values of 3% for hydrophobic BC and 20% for hydrophilic BC, given that total BC is a combination of the two. Leaving all BC in the surface snow with melt ( $s_B=0\%$ ) as done in the *Rypdal et al.* [2009] and *Skeie et al.* [2011] model studies would lead to overestimates of surface snow BC during the melt period.

## 5. Results for Greenland

[51] In the percolation zone of the Greenland ice sheet only a fraction of the annual snow accumulation melts during the

summer season. Therefore the summertime surface layer is buried each year by new snowfall and, when new snow is sufficiently deep, the layer with melt-amplified ILAP concentrations no longer affects surface albedo. However, snow with amplified concentrations of ILAP will remain at depth in the snowpack. Near Dye-2, where our measurements were made, new snow falls occasionally in the summer, reducing the albedo effect of surface melt amplification (Figure 1). A vertical profile through the snowpack corresponds to sampling backward in time, and we expect that buried layers of enhanced particulate concentrations correspond to summer layers of earlier years.

[52] We were able to observe several years’ snow accumulation, including summertime melt layers. Figure 7 shows the stratigraphic structure of the snowpack, indicating where different types of snow and the ice layers were found in the 2 m (pit 1) and 1 m (pit 2) deep profiles. Figure 8 shows  $L$  and  $\hat{a}_{\text{abs}}$  as functions of snow depth for the two snow pits. Three summertime melt layer peaks in  $L$  are apparent, at the snow surface and at approximately 60 cm and 160 cm depth.  $\hat{a}_{\text{abs}}$  (Figure 8b) varied between minima of  $\sim 1.2$ – $1.4$  and maxima of  $\sim 2.5$ – $3.0$ , with a rapid transition as one moves forward in time (upward in the snowpack) from the maxima to the minima. This indicates a rapid seasonal change in the source of light-absorbing particles to snow in this region. Sampling was done in late July, and at that time the surface snow  $\hat{a}_{\text{abs}}$  was near its annual minimum (Figures 8b and 9b), indicating that the rapid transition in  $\hat{a}_{\text{abs}}$  occurred in early to

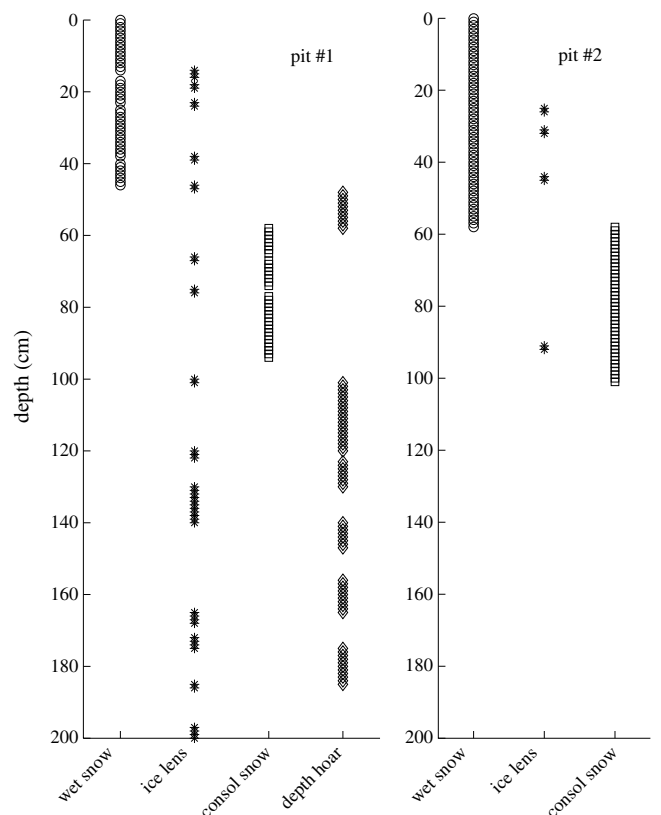


**Figure 7.** Snow stratigraphy in the percolation zone of the Greenland ice sheet. Depths of the different types of snow (wet snow, consolidated frozen snow, and depth hoar) and ice layers are shown for the two snow pits near Dye-2.

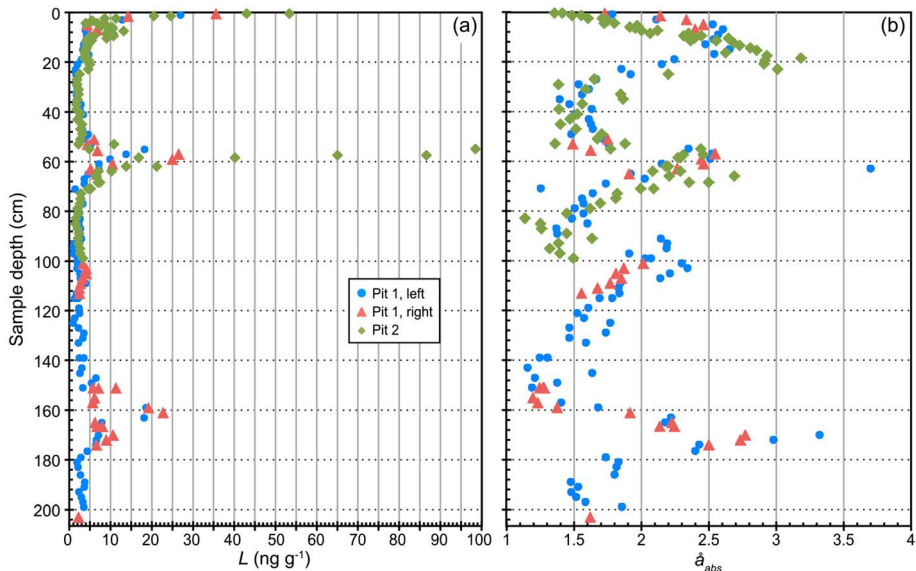


**Figure 8.** Vertical profiles near Dye-2, Greenland, in July 2010 of (a)  $L$  and (b)  $\hat{a}_{abs}$ . This full profile corresponds to approximately four years' worth of snow accumulation, as can be seen from the four seasonal cycles in  $\hat{a}_{abs}$ . The profile of  $L$  also shows a seasonal cycle, with the peak in the top  $\sim 10$  cm of the snow corresponding to summer 2010, and peaks centered at approximately 60 and 160 cm depth corresponding to melt amplification peaks in the summers of 2009 and 2007, respectively. A summertime peak for 2008 (at approximately 115 cm depth) is missing in the plot of  $L$ , but the 2008 peak in  $\hat{a}_{abs}$  is present. Data are shown separately for the left and right profiles in the first snow pit; for the second snow pit, data from the left and right profiles are shown using the same symbol.

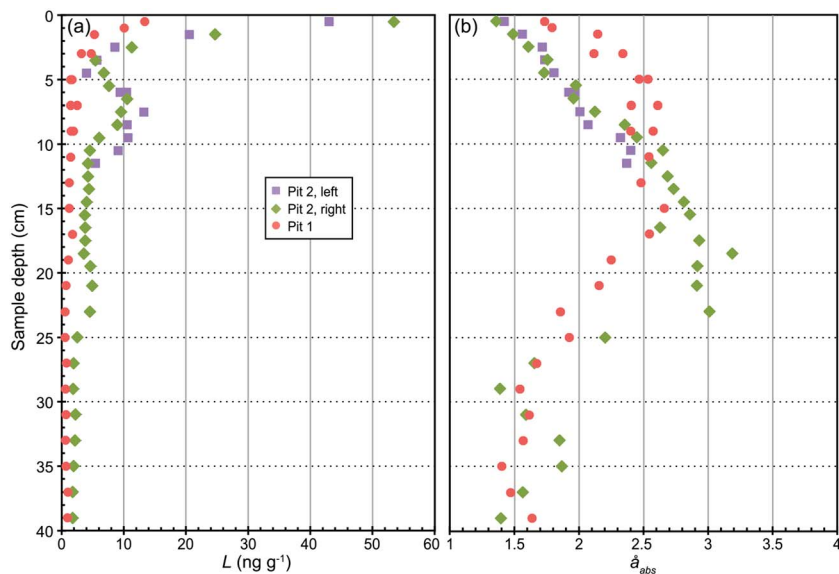


**Figure 9.** As in Figure 8, but focusing on just the topmost 40 cm of the snowpack, corresponding to the 2009–2010 winter (deeper snow) through July 2010 (surface snow). Samples from pit 2 have 1 cm vertical resolution in the top 20 cm of the snowpack (purple squares and green diamonds), revealing finer structure to the surface snow concentrations of light-absorbing particles. Data from the first snow pit (red dots; sampled at 2 cm resolution) do not show this same structure.

mid-summer and that low values of  $\hat{a}_{abs}$  correspond to mid to late summer, autumn and perhaps early winter deposition. Higher values of  $\hat{a}_{abs}$  likely correspond to deposition in later winter and early spring, but without information on snow accumulation, compaction and total melt rates throughout the year it is not possible to associate the

variations in  $\hat{a}_{abs}$  to exact times of the year. Lower values of  $\hat{a}_{abs}$  are generally associated with fossil fuel combustion and higher values with biomass burning [Rosen *et al.*, 1978; Bond *et al.*, 1999; Bond, 2001; Clarke *et al.*, 2004; Bergstrom *et al.*, 2007; Kirchstetter *et al.*, 2004], so the observed annual cycle is generally consistent with a winter/

spring biomass burning source and a summertime fossil fuel source. Indeed, in a source attribution study based on the chemical composition of the snow, *Hegg et al.* [2009; 2010] found that biomass burning was the primary source of ILAP to snow at Dye-2 in the winter and spring, but in the summer the primary source was pollution (fossil fuel burning).

[53] The apparent annual cycle in  $\hat{a}_{\text{abs}}$  has four peaks, implying that there is a year of “missing” amplification in  $L$  at  $\sim 100$  cm depth. Thus we conclude that this profile encompasses summer melt layers from 2010 (surface), 2009 (60 cm), 2008 (100 cm), and 2007 (160 cm). In section 5.1, we provide further justification for this conclusion.

[54] The peak in  $L$  in the buried (2009 and 2007) layers appears to have been displaced lower in the snowpack relative to the minima in  $\hat{a}_{\text{abs}}$  than is the surface (2010) peak. We show below that only about half the total melt for summer 2010 had occurred when we made our measurements. At Barrow, we noted that the initially low values of  $\hat{a}_{\text{abs}}$  at the snow surface increased as the snow melted, consistent with the preferential wash down of low  $\hat{a}_{\text{abs}}$  particles (i.e., BC). At Dye-2, it appears that particles with low  $\hat{a}_{\text{abs}}$  are deposited to the snow in mid to late summer, but the process of melting removes a significant fraction of these particles from the surface snow, and as the low  $\hat{a}_{\text{abs}}$  layer is removed with melt, the surface progressively includes more particles from snow that fell earlier in the year, when  $\hat{a}_{\text{abs}}$  of deposited particulates was higher. Therefore it again appears the BC is scavenged more efficiently with meltwater than are the other light-absorbing particulates.

[55] Identification of peaks in  $L$  as melt layers, and therefore summers in specific years, is based on the assumption that these peaks are not due to increased summertime deposition of light-absorbing particles. Newly fallen snow samples from 1 May to 1 July 2010 can be used to test this assumption.  $L$  for these samples was  $7.5 \pm 3.5$  ng/g, versus  $>20$  ng/g in the peaks. (A newly fallen snow sample from 22 July 2008 had much lower concentrations, 0–2 ng  $\text{g}^{-1}$ ; Figure 1).  $L$  for the 2010 new snow and for the samples at  $\sim 5$ –10 cm depth in pit 2 are about a factor of 2 higher than in samples from deeper in the snow (i.e., earlier in the year; Figure 9), so some of the increase in  $L$  in the late spring/early summer versus in winter could be due to increased deposition. However, deposition cannot account for the much higher concentrations observed in the surface melt layers.

[56] A smaller peak in  $L$  is seen immediately below the summer snow melt layer in 2010 in pit 2 (Figure 9a), but it is not apparent at pit 1, nor is it seen in the sections of the profile corresponding to previous years’ summers. In the latter case, this could be because melt was sufficient that this smaller peak was subsumed into the melt layer peak. By the end of the summer, the snowpack likely melted sufficiently to subsume the 5–10 cm depth peak in  $L$ . Also important to remember is that deeper snow may be affected by infiltration of melting snow and by vapor redistribution (i.e., hoar-frost formation), both of which affect  $L$  and may be obscuring variations which existed when the snow was at the surface. At Summit, Greenland, where the snow remained below freezing year-round, *Hagler et al.* [2007] observed a seasonal cycle in the concentration of BC in falling snow, with about a factor of two decrease from late May to late June and into July (see their Figure 6). This is consistent with the small buried peak we observe at Dye-2 in 2010

and also with the strong summertime peak being associated with melt amplification, not increased deposition.

### 5.1. The Disappearing Summer of 2008

[57] As noted above, there is no peak in  $L$  at the depth ( $\sim 100$  cm) that we believe corresponds to summer 2008. Coincidentally, we have a vertical profile of estimated BC concentrations ( $B$ ) in snow samples collected near Dye-2 during summer 2008, and this profile also includes a melt layer (Figure 1). The 2008 profile shows concentrations ( $B$ ) of up to 20 ng  $\text{g}^{-1}$  in the melt layer and about 1 ng  $\text{g}^{-1}$  below this. New snow fell on the day preceding the measurements, and the new snow on top of the melt layer also had concentrations,  $B$ , of  $\sim 1$ –2 ng  $\text{g}^{-1}$ . Thus, clearly there was amplification of BC and other light absorbers in 2008 in the surface melt layer, but for some reason that peak was lost by 2010 due to in-snow processing.

[58] To try to understand why 2008 might differ from other years we looked to snow depth and surface air temperature data from an automatic weather station (AWS) near Dye-2 and, because there are large gaps in the Dye-2 AWS data, also from the AWSs at the “Saddle” and “NASA-SE” sites. These sites are  $\sim 100$ –150 km to the east of Dye-2 and at somewhat higher elevation, but relative interannual variations in gross climatic parameters should be qualitatively similar at all three, especially since they are at similar latitude.

[59] Figure 10 shows relative snow depth from all three stations for the times when data are available. Each year’s data are shown relative to the average depth from days 128 to 146 (8–26 May) of that year. Increases are always due to snowfall, but decreases can be a combination of compaction, sublimation and melting. There is considerable interannual variability in timing of the melt season and amount of melt. These data show that at Dye-2 the snow depth in 2007 declined during summer by about 40 cm, whereas in 2008 there was almost no summertime decrease in snow depth. In 2010, at the time our measurements were made total snow depth had decreased by 15 cm from its peak value, but by day 240 (end of August) snow depth had declined a further 15 cm. In other words: at the time of our measurements, (a) only about half the total summertime melt had occurred, (b) the 2010 total melt was probably only moderately less than that in 2007, and (c) melt in 2007 and 2010 appears to have been much greater than in 2008. AWS snow depth and surface air temperature data are not available for 2009 at Dye-2, but the data from NASA-SE show similar snow-depth trends for 2009 and 2010 (here, data for 2008, and most of 2007 are not available). At the Saddle AWS there was considerably more melt in 2007 than in 2008 (here, data for 2009 and 2010 are not available).

[60] Another metric of the intensity of melt is the number of 1 h resolution surface air temperature,  $T_{\text{air}}$ , reports with  $T_{\text{air}}$  above some near-freezing threshold. Temperature thresholds of  $-2^\circ\text{C}$ ,  $0^\circ\text{C}$ , and  $+2^\circ\text{C}$  all yield similar results: at Dye-2, there were about 25% more days in 2007 than in 2010 when these temperatures were reached, but in 2008 only about half as many days as in 2010. Saddle shows a comparable number of days in 2007 and 2010 when these  $T_{\text{air}}$  thresholds were exceeded, but about a quarter (for  $T_{\text{air}} > 0^\circ\text{C}$ ) or half (for  $T_{\text{air}} > -2^\circ\text{C}$ ) as many instances in 2008. At NASA-SE, there were about twice as many days in 2010 that reached these temperature thresholds than in

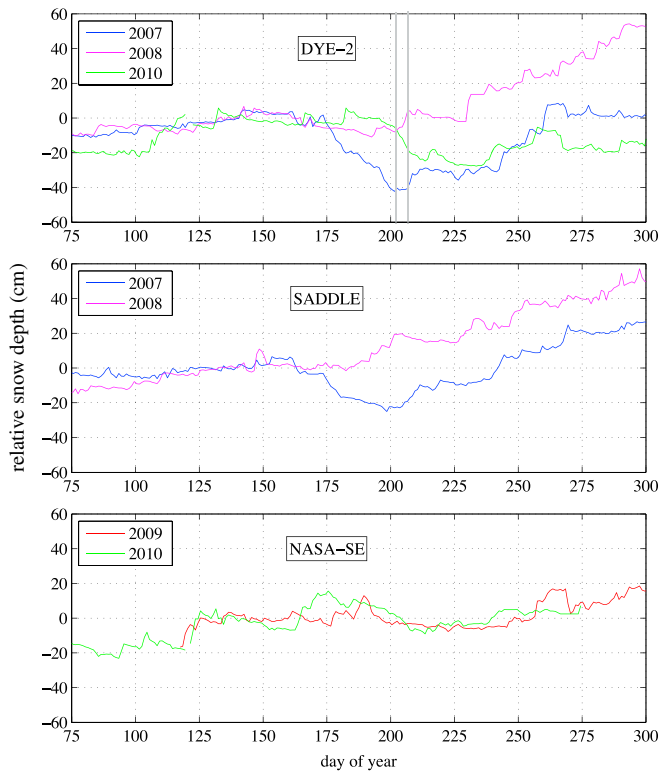


**Figure 10.** Relative snow depth as a function of day of year for years 2007–2010, as available from Automatic Weather Stations at three sites on the Greenland Ice sheet: Dye-2 ( $66^{\circ}28.83'N$ ,  $46^{\circ}16.98'W$ , 2099m), Saddle ( $65^{\circ}59.98'N$ ,  $44^{\circ}30.10'W$ , 2467m), and NASA-SE ( $66^{\circ}28.50'N$ ,  $42^{\circ}29.92'W$ , 2373m). All depths are relative to the average snow depth at the station on days 128–146 (8–26 May). Vertical gray lines in the Dye-2 plot indicate the sampling start and end dates for the data shown in Figures 8 and 9; the right-hand vertical gray line also corresponds to the date of the single snow profile taken near Dye-2 in 2008 (AWS data courtesy Konrad Steffen research group, CIRES).

2007 and 2009, but this may not be statistically significant as these temperatures were, in general, not often reached at that station (hence, the very small declines in snow depth, bottom panel of Figure 10).

[61] Taken together, the snow depth and temperature data indicate that there was considerably less melting—perhaps about half as much—in 2008 as in 2007, 2009, and 2010. However, we did observe a melt peak in the samples collected in July 2008 and we cannot explain why that peak was not preserved at depth in 2010.

## 5.2. ILAP and BC Amplification Factors

[62] At Dye-2, amplification factors are calculated for both  $L$  and  $B$  ( $A_L$  and  $A_B$ , respectively) for the melt layer from summer 2010. As noted above, concentrations in the late spring/early summer snow appear to be about twice those from earlier in the year (i.e., from deeper in the snowpack). Therefore we calculate amplification factors (Table 4) relative to the average concentration in the 2010 new snow samples ( $B = 5.6 \text{ ng g}^{-1}$ ;  $L = 7.5 \text{ ng g}^{-1}$ ) and also relative to the average concentration in the “subsurface”

**Table 4.** Amplification Factors for the Concentration of Light-Absorbing Particles in Surface Snow During the 2010 Melt Season Near Dye-2<sup>a</sup>

	Amplification Factors			
	(a) Relative to subsurface snow		(b) Relative to 2010 new snow	
	$A_L$	$A_B$	$A_L$	$A_B$
<b>Pit 1, 2010</b>				
Top 1 cm	13.3	14.4	4.7	5.6
Top 2 cm	9.6	10.2	3.4	4.0
Top 4 cm	7.3	7.7	2.6	3.0
Top 10 cm	4.3	4.4	1.5	1.7
<b>Pit 2, 2010</b>				
Top 1 cm	16.3	19.2	6.4	7.8
Top 2 cm	12.0	14.0	4.7	5.7
Top 4 cm	7.3	8.5	2.9	3.5
Top 10 cm	4.7	5.3	1.9	2.2

<sup>a</sup>Calculated as the ratio of the mixing ratios in the top 1, 2, 4 or 10 cm of the snowpack to (a) that in the subsurface snow (5–25 cm deep) or (b) the average from newly fallen snow collected at Dye-2 from 1 May to 1 July 2010. Amplification factors are given for both all ILAP ( $A_L$ ) and for estimated BC ( $A_B$ ). These values apply to measurements in late July 2010, when about half the full summer melt had occurred.

snow ( $B = 2.3 \text{ ng g}^{-1}$ ;  $B = 3.0 \text{ ng g}^{-1}$ ; corresponds to data in Figure 8a; Table 4).

[63] Amplification is strongest at the very surface of the snowpack about three times that for the top 10 cm. For the given snow density and ILAP concentrations in this melting snowpack, the  $e$ -folding depth of mid-visible sunlight is 3–10 cm snow depth (equivalent to 1–3 cm liquid-equivalent depth) [King and Simpson, 2001; France et al., 2012; Reay et al., 2012], so albedo reduction will relate more closely to the average amplification factors over 4–10 cm depth. Amplification factors relative to the newly fallen snow are about half those relative to the concentrations deeper in the snowpack, so that averaged over the top 10 cm of the snow concentrations are roughly only doubled by melt amplification. The profile from pit 2 (Figure 9a) appears not to have melted sufficiently to have incorporated ILAP from the high-concentration early summer snow, so amplification factors relative to the new snow concentrations should more accurately reflect the degree to which BC and other light absorbers in surface snow are retained near the surface with melt. On the other hand, concentrations in pit 1 drop rapidly below the melt layer, indicating that a comparison with subsurface “baseline” concentrations is more appropriate. The full summer’s melt at this site is sufficient to subsume both the higher concentration late spring/early summer snow and the lower concentration snow from earlier in the spring and late winter. The buried peaks from previous years’ melt will therefore include the influence of both, but they also have likely been altered by in-snow processing and ILAP redistribution post-burial.

## 5.3. ILAP Scavenging Efficiencies

[64] The data from Dye-2 are a snapshot of the snowpack at a point in time after a significant amount of melting had occurred. Using the AWS snow height data, we can approximate the total snow depth change from before the onset of melt (on approximately 14 July 2010) to when we

sampled the surface snow. Snow height decreased by about 9 cm between 14 and 21 July (site 1 sampling) and another 7 cm by 24 July (site 2 sampling), with part of the latter due to compaction from a rain event on 22 July. As noted above, equation (2) is convergent for a sufficient number of steps,  $n$ , i.e., for a sufficient amount of melt. Surface snow concentrations at the two sites are very similar despite there having been significant additional snow loss to melt between 21 and 24 July. This indicates that sufficient melting has likely occurred for  $m_L'$  to approximately reach its convergent value.

[65] At Dye-2, amplification of ILAP is apparent in the top 4 cm of the snowpack, so here  $m_L$  and  $m_L'$  are for a 4 cm deep column, and these are in turn used to calculate  $s_L$  (equation (2)). As at Barrow,  $s_L$  is calculated for a range of values of  $m_L$  and  $m_L'$ .  $m_L$  is calculated using  $L$  values of 3–8 ng g<sup>-1</sup> (corresponding to the range of concentrations in sub-surface and late spring/early summer snow fall events) and a snow density of 350 kg m<sup>-3</sup>, appropriate for wind-compacted snow [Albert and Hawley, 2002]. Values of  $m_L'$  are calculated using  $L$  in the top 4 cm of the snowpack in pits 1 and 2, which were 20 and 22 ng g<sup>-1</sup> respectively, so we calculate  $s_L$  for  $m_L'$  corresponding to  $L$  of 20–24 ng g<sup>-1</sup> and the measured melt layer snow density of 400 kg m<sup>-3</sup>. Melt scavenging rates for BC,  $s_B$ , are not calculated for this data set; uncertainty in the range of appropriate values for  $m_B$  would be even larger than for  $m_L$  because of the additional uncertainty in apportioning total absorption to BC and non-BC constituents, especially given the strong vertical variations in  $\hat{a}_{\text{abs}}$  of snow particulates (Figure 8b).

[66] Estimates of  $s_L$  are ~10–40% (Table 5). As noted above, concentrations deeper in the snowpack, corresponding

to snowfall from winter and possibly early spring, are lower ( $L \sim 3$  ng g<sup>-1</sup>) than in the late spring/early summer snowfall ( $\sim 7$  ng g<sup>-1</sup>). We expect that the melt layer observed in our late July measurements was more strongly influenced by the latter than the former. As the most appropriate estimate, we therefore take  $L$  of unmelted snow as 5–7 ng g<sup>-1</sup> and infer  $s_L$  in the range 20–30%. This is somewhat higher than the best estimate range for  $s_L$  from Barrow (~10–20%; Table 3). This could be due to a difference in the composition of the ILAP at the two sites or an underestimate in  $s_L$  at Barrow if there was not sufficient melting for  $m_B$  to have reached its asymptotic value, or a combination of the two.

## 6. Results for Tromsø, Norway

[67] At Tromsø, six successive days' measurements in 2008 show amplification of concentrations of light-absorbing particles in surface snow with melting (21–30 May) (Figure 11 and Table 6). In this region, the terrain was hummocky, with bushes and smaller shrubs. On successive measurement days, the previous days' sampling site was sometimes found to be snow-free, so each day a new sampling site was selected within 10 m of the previous sampling site. Although the snow was melting rapidly, total snow depth in our profiles does not systematically decline because each day a sampling location was chosen that still contained deep snow. Therefore  $L$  and  $\hat{a}_{\text{abs}}$  are plotted relative to the fraction of total snowpack depth within a given profile.

[68] Amplification factors ( $A_L$  and  $A_B$ ) are calculated relative to the average subsurface snow concentrations within each profile. As at Barrow and Dye-2, the surface snow concentrations increase as the snow melts (Table 6 and Figure 11). Amplification factors for the top 3 cm of the snowpack are about 2–3 by the end of the measurements. Here there is no apparent trend in  $\hat{a}_{\text{abs}}$  in the layer of melt amplification, indicating similar scavenging rates for BC and non-BC ILAP.

[69] The profile from 30 May has anomalously high values of  $L$  (Figure 11a) and high values of  $\hat{a}_{\text{abs}}$  throughout the snowpack, which we cannot explain. The profile from 28 May also has anomalously high values of  $\hat{a}_{\text{abs}}$  in the bottom three quarters of the snowpack, but the surface snow values were consistent with those on early days. Thus, care should be taken in comparing successive days' profiles.

**Table 5.** The ILAP Scavenging Factors,  $s_L$ , for Sites 1 and 2 Near Dye-2, Greenland (as in Table 3 for Barrow), for a Range of Assumed Concentrations in the Snow Before and After Melt

$s_L$	$L$ , Unmelted Snow (ng g <sup>-1</sup> ):					
	3	4	5	6	7	8
<b>18</b>	14%	20%	24%	29%	34%	38%
<b>20</b>	13%	18%	<b>22%</b>	<b>26%</b>	<b>30%</b>	34%
<b>22</b>	12%	16%	<b>20%</b>	<b>24%</b>	<b>28%</b>	32%
<b>24</b>	11%	14%	18%	22%	26%	29%

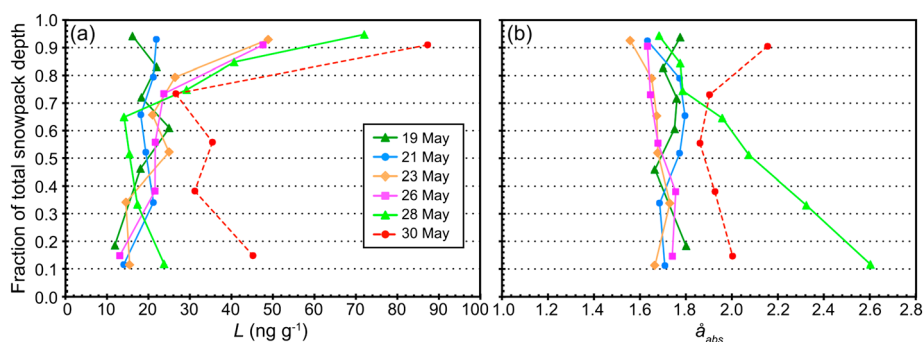


**Figure 11.** Profiles of (a)  $L$  and (b)  $\hat{a}_{\text{abs}}$  from spring, 2008 near Tromsø, Norway. The 19 and 21 May profiles precede the onset of melt; from 23 May onward the snowpack was melting. Spatial variability in total snowpack depth across the sampling region was high, so data are plotted as a function of the ratio of snow sample depth to total snowpack depth in a given profile.

**Table 6.** Concentrations and Amplification Factors for All ILAP ( $L$  and  $A_L$ , Respectively) and for BC ( $B$  and  $A_B$ ) in the Mountain Snowpack Near Tromsø, Norway in 2008<sup>a</sup>

Date	Total Snow Depth (cm)	$L$ (ng g <sup>-1</sup> )				Amplification Factors	
		Top 3 cm		Top 3 cm		$A_L$	$A_B$
		Subsurface	Subsurface	Subsurface	Subsurface		
19 May	27	16.	19	14	17	0.9	0.9
21 May	22	22	19	19	16	1.2	1.2
23 May	22	49	20	44	18	2.4	2.5
26 May	17	48	20	43	17	2.4	2.4
28 May	30	72	23	64	19	3.1	3.3
30 May	17	87	35	72	29	2.5	2.5

<sup>a</sup>Surface values are for the top 3 cm of the snowpack; sub-surface values are averages of all samples below 3 cm. On 19 and 21 May the snowpack was still below freezing, but by 23 May it had started to melt. Temperatures through 30 May were sufficient for continued melting.

**Table 7.** The  $L$ ,  $\hat{a}_{\text{abs}}$ , and Amplification Factors for all ILAP ( $A_L$ ) in the Mountain Snowpack Near Tromsø, Norway on three Days in 2010<sup>a</sup>

Date	Sample Depth (cm)	$\hat{a}_{\text{abs}}$	$L$	$A_L$
15 May	0–3	2.4	70	4.1
	3–6	2.1	20	
	6–9	1.8	15	
	9–14	2.6	48	
18 May	0–3	2.0	51	2.0
	3–6	1.8	27	
	6–9	2.2	24	
	9–33	2.5	35	
21 May	0–3	2.2	236	4.8
	3–6	2.2	44	
	6–9	2.6	55	
	9–22	2.4	105	

<sup>a</sup>In all three profiles the snow had been actively melting for several days.

[70] Measurements were also made at Tromsø in a second spring season, on three days in 2010 (Table 7). The snow had been melting for several days before the first measurements were made on 15 May, so we do not have a profile of ILAP unaffected by melt. Each profile was taken from a different location on the mountain because the snowpack at the previous sampling site had completely melted in the interim, so sample sites are from locations with particularly deep snow (i.e., depressions). This likely explains the higher values of  $L$  in the bottom-most samples: the snow there may be mixed with local soil. Amplification factors for ILAP are shown (Table 7) as the ratio of the surface (0–3 cm) to subsurface (3–9 cm) values of  $L$  and are comparable to those from 2008 and also comparable to those from the 2010 Dye-2 values for the top 4 cm, when compared to concentrations in new snow (Table 4, column b).

## 7. Discussion and Conclusions

[71] BC and other insoluble light-absorbing particulate (ILAP) concentrations in surface snow increase with melt because their scavenging efficiency with snow meltwater is less than 100%. To better constrain how this affects surface snow concentrations, measurements were made at three

sites during their melt seasons. Amplification factors are presented for  $L$ , a proxy for all ILAP, and for estimated BC concentrations,  $B$ , in melting surface snow. Melt scavenging efficiencies for all ILAP and for BC,  $s_L$ , and  $s_B$ , are also presented.

[72] Within a few days of active melting, BC and total ILAP concentrations in the top 2 cm of the snowpack were observed to increase by about factors of 4.5 and 5.5, respectively, for snow on sea ice near Barrow, Alaska (Table 2b). At a site near Dye-2, Greenland, amplification factors were similar to Barrow when melting snow is compared to newly fallen snow in late spring and early summer, but were even higher (~10–15) when compared to concentrations in the snow from earlier in the year (Table 4). At a site near Tromsø, Norway, somewhat lower amplification factors were observed (factor of ~2–3).

[73] Amplification of BC and other ILAP concentrations appears to be largely confined to the top 2–4 cm of the snowpack during melt. Depending on snow grain size and density (and on impurity content), the spectrally integrated penetration depth of sunlight is ~3–10 cm so calculations of albedo reduction due to melt amplification need to account for the decline in amplification with depth. At the Barrow sampling site, amplification for the top 4 cm was about 80% that for the top 2 cm. At the Dye-2 site, amplification for the top 4 cm was about 70% that for the top 2 cm; in the top 10 cm, it was about 40% that for the top 2 cm.

[74] The ILAP scavenging efficiencies were calculated based on the assumption that with each increment of melt, a fraction of the melting surface snow ILAP is left behind and added to the snowpack in the remaining surface layer. For scavenging efficiencies of >0%, the process results in amplification factors that reach an asymptotic value after sufficient melt. For scavenging efficiencies ( $s$ ) of 5%, 10%, 15%, 20%, and 30% the amplification factors asymptote to ~16, 10, 7, 5, and 3, respectively. Using this model, melt scavenging efficiencies were calculated for the Barrow and Dye-2 data sets. For the Barrow data set, we determined a melt scavenging efficiency for the aggregate of all particulate light absorbing impurities ( $s_L$ ) as well as for BC alone ( $s_B$ ). Estimates of  $s_B$  were a few percent lower than for  $s_L$ , but given the accuracy of our measurements it appears that both BC and non-BC light-absorbing constituents are removed from the snowpack with melt with roughly equal efficiency. This result could be explained if all absorbers usually occur together in the same particles as an “internal mixture,” so that removal rates are determined more strongly by the particle size distribution and total particle solubility rather than by the size and solubility of individual components.

[75] Our best estimates of the scavenging efficiency with snow meltwater of both BC ( $s_B$ ) and all ILAP ( $s_L$ ) from field measurements at Barrow (~10–20%) and Dye-2 (~20–30%) are consistent with the values used by *Flanner et al.* [2007] for BC alone in a model study, where it was assumed that  $s_B$  is 3% for the hydrophobic BC and 30% for hydrophilic BC. The fraction of hydrophobic versus hydrophilic BC in the snow varies in the model with location but is not specified by *Flanner et al.* [2007], precluding a direct comparison of typical melt scavenging efficiencies for all BC in the model. The model studies of *Rypdal et al.* [2009] and *Skeie et al.* [2011] assume that all BC remains in the snowpack with melt, so these models underestimate the amount of BC

washed down with melt. This will lead to an overestimate in the melt amplification feedback to radiative forcing by BC in snow. In contrast, other models do not account for melt amplification and so miss this positive feedback process altogether.

[76] Surface snow amplification of BC and other ILAP can be large, especially once the snow is rapidly melting, but this may not translate directly into large reductions in surface albedo. For seasonal snow, during melt the snowpack is also thinning and, once sufficiently thin, the albedo of the underlying surface (e.g., land/vegetation, ice) will start to influence the surface albedo more than the snow impurities. Determining at what point this happens depends on snow depth and structure, and especially on the small-scale horizontal variations of snow thickness due to scouring and drifting. Furthermore, the time period over which surface albedo is reduced by melt amplification can be short. At Barrow, the transition from a cold snowpack at its seasonal maximum depth to an almost fully melted snowpack took only about three weeks, and surface snow concentrations of ILAP were significantly amplified only during the last four days of our observations. In central Greenland, where the snow is on an ice sheet, the melting of seasonal snow does not expose a dark underlying surface as occurs when seasonal snow is on earth. Thus, surface albedo reduction here is driven purely by changes in snowpack morphology and impurity concentrations. In addition, periodic new snowfall events, which can occur even in the summer in Greenland, bury layers of melt-amplified concentrations, reducing their effect on albedo.

[77] None of the measurements were made in locations where soil or mineral dust are expected to be present in significant quantities. On many mountain glaciers, soil/dust likely dominate particulate light absorption in snow [Painter *et al.*, 2007, 2012]. In some locations, such as western China, BC deposition is maximized when dust deposition is also high [Ming *et al.*, 2009]. As shown by Conway *et al.* [1996], coarse particles such as volcanic ash remain at the snow surface with melt with much higher efficiency than even hydrophobic smaller particles. Therefore in snowpacks where particulate light absorption is dominated by soil and mineral dust these constituents will rapidly accumulate on the snow surface. Indeed, this can lead to fully debris-covered surfaces on glaciers where melt initially is accelerated by the presence of impurities; however, when the debris layer thickness reaches 2–3 cm it acts as an insulating barrier between the glacial snow/ice and the atmosphere and slows glacial melt [Østrem, 1959; Driedger, 1981; Rhodes *et al.*, 1987, and references therein]. In addition, in snow with a high dust-to-BC ratio, the relatively lower meltwater scavenging efficiency for dust versus BC means that dust will play an increasingly dominant role in snow albedo reduction during the melt season, so forcing by a given concentration of BC is reduced.

[78] **Acknowledgments.** We thank Drew Abbott and Silver Williams for collecting samples of individual snowfall events at Dye-2 (Raven Camp) from April to July 2010 and for hosting us at Raven Camp; Lou and Mark Albershardt for hosting us at Raven Camp in 2008; Kathleen Huybers for assisting with melting and filtering of samples in Greenland; and Ryan Eastman for assisting with field and laboratory work at Barrow. The Barrow Arctic Science Consortium (BASC) provided logistical support in Barrow. We thank Konrad Steffen's Research Group at the Cooperative Institute for Research in Environmental Sciences (CIRES) at the University of Colorado for providing the Greenland AWS

data. We also thank Song Gao and Stephanie Munroe of Nova University for performing the IC analysis on the Barrow samples. We thank Florent Dominé and two anonymous reviewers for their careful reading of the paper and their helpful comments. This work was funded by the U.S. National Science Foundation grant NSF-ARC-06-12626 and the U.S. Environmental Protection Agency STAR grant RD-83503801. Sampling in Tromsø was funded by the Research Council of Norway under project 165064/S30 (Climate effects of reducing black carbon emissions), 178912/S30 (Measurements of black carbon aerosols in Arctic snow—Interpretation of effect on snow reflectance) and 184724/S30 (Variability of albedo using an unmanned aerial vehicle).

## References

- Aamaas, B., C. E. Bøggild, F. Stordal, T. Berntsen, K. Holmén, and J. Ström (2011), Elemental carbon deposition to Svalbard snow from Norwegian settlements and long-range transport, *Tellus*, *63B*, 340–351, doi:10.1111/j.1600-0889.2011.00531.x.
- Albert, M. R., and R. L. Hawley (2002), Seasonal changes in snow surface roughness characteristics at Summit, Greenland: implications for snow and firn ventilation, *Ann. Glaciol.*, *35*, 510–514.
- Bergstrom, R. W., P. Pilewskie, P. B. Russell, J. Redemann, T. C. Bond, P. K. Quinn, and B. Sierau (2007), Spectral absorption properties of atmospheric aerosol, *Atmos. Chem. Phys.*, *7*, 5937–5943.
- Bond, T. C., M. Bussemer, B. Wehner, S. Keller, R. J. Charlson, and J. Heintzenberg (1999), Light absorption by primary particle emissions from a lignite burning plant, *Environ. Sci. Technol.*, *33*, 3887–3891.
- Bond, T. (2001), Spectral dependence of visible light absorption by carbonaceous particles emitted from coal combustion, *Geophys. Res. Lett.*, *28*, 4075–4078.
- Bond, T. C., and R. W. Bergstrom (2006), Light absorption by carbonaceous particles: An investigative review, *Aerosol Sci. Tech.*, *40*, 27–67.
- Clarke, A. D., and K. J. Noone (1985), Soot in the Arctic snowpack—A cause for perturbations in radiative transfer, *Atmos. Environ.*, *19*(12), 2045–2053, doi:10.1016/0004-6981(85)90113-1.
- Clarke, A. D., et al. (2004), Size distributions and mixtures of dust and black carbon aerosol in Asian outflow: Physicochemistry and optical properties, *J. Geophys. Res.*, *109*, D15S09, doi:10.1029/2003JD004378.
- Clarke, A., et al. (2007), Biomass burning and pollution aerosol over North America: Organic components and their influence on spectral optical properties and humidification response, *J. Geophys. Res.*, *112*, D12S18, doi:10.1029/2006JD007777.
- Conway, H., A. Gades, and C. F. Raymond (1996), Albedo of dirty snow during conditions of melt, *Water Resour. Res.*, *32*(6), 1713–1718.
- Doherty, S. J., S. G. Warren, T. C. Grenfell, A. D. Clarke and R. E. Brandt (2010), Light-absorbing impurities in Arctic snow, *Atmos. Chem. Phys.*, *10*, 11647–11680, doi:10.5194/acp-10-11647-2010.
- Driedger, C. L. (1981), The 1980 eruptions of Mount St. Helens, Washington. Effect of ash thickness on snow ablation, U. S. Geological Survey, *Professional Paper 1250*, 757–760.
- Flanner, M. G., C. S. Zender, J. T. Randerson and P. J. Rasch (2007), Present-day climate forcing and response from black carbon in snow, *J. Geophys. Res.*, *112*, D11202, doi:10.1029/2006JD008003.
- Flanner, M. G., C. S. Zender, P. G. Hess, N. M. Mahowald, T. H. Painter, V. Ramanathan and P. J. Rasch (2009), Springtime warming and reduced snow cover from carbonaceous particles, *Atmos. Chem. Phys.*, *9*, 2481–2497, doi:10.5194/acp-9-2481-2009.
- France, J. L., M. D. King, J. Lee-Taylor, H. J. Beine, A. Ianniella, F. Domine, and A. MacArthur (2011), Calculations of in-snow NO<sub>2</sub> and OH radical photochemical production and photolysis rates: A field and radiative-transfer study of the optical properties of Arctic (Ny-Ålesund, Svalbard) snow, *J. Geophys. Res.*, *116*, doi:10.1029/2011JF002019.
- France, J. L., H. J. Reay, M. D. King, D. Voisin, H. W. Jacobi, F. Domine, H. Beine, C. Anastasio, A. MacArthur, and J. Lee-Taylor (2012), Hydroxyl radical and NO<sub>x</sub> production rates, black carbon concentrations and light-absorbing impurities in snow from field measurements of light penetration and nadir reflectivity of onshore and offshore coastal Alaskan snow, *J. Geophys. Res.*, *117*, D00R12, doi:10.1029/2011JG016639.
- Grannas, A. M., et al. (2007), An overview of snow photochemistry: Evidence, mechanisms and impacts, *Atmos. Chem. Phys.*, *7*, 4329–4373.
- Grenfell, T. C. (1992), Surface-based passive microwave studies of multiyear sea ice, *J. Geophys. Res.*, *97*(C3), 3485–3501.
- Grenfell, T. C., S. J. Doherty, A. D. Clarke, and S. G. Warren (2011), Light absorption by particulate impurities in snow and ice determined by spectrophotometric analysis of filters, *Appl. Opt.*, *50*, 2037–2048.
- Hagler, G. S. W., M. H. Bergin, E. A. Smith, J. E. Dibb, C. Anderson, and E. J. Steig (2007), Particulate and water-soluble carbon measured in recent snow at Summit, Greenland, *Geophys. Res. Lett.*, *34*, L16505, doi:10.1029/2007GL030110.

- Hansen, J., and L. Nazarenko (2004), Soot climate forcing via snow and ice albedos, *Proc. Natl. Acad. Sci. USA*, *101*(2), 423–428, doi:10.1073/pnas.2237157100.
- Hegg, D. A., S. G. Warren, T. C. Grenfell, S. J. Doherty, T. V. Larson, and A. D. Clarke (2009), Source attribution of black carbon in snow, *Env. Sci. Tech.*, *43*(11), 4016–4021, doi: 10.1021/es803623f.
- Hegg, D. A., S. G. Warren, T. C. Grenfell, S. J. Doherty, and A. D. Clarke (2010), Sources of light absorbing aerosol in arctic snow and their seasonal variability, *Atmos. Chem. Phys.*, *10*, 10923–10938, doi:10.5194/acp-10-10923-2010.
- Higuchi, K., and A. Nagoshi (1977), Effect of particulate matter in surface snow layers on the albedo of perennial snow patches, in *Isotopes and Impurities in Snow and Ice*, Proc. of the Grenoble Symposium, IAHS AISH Publ., *118*, 95–97.
- Honrath, R. E., Y. Lu, M. C. Peterson, J. E. Dibb, M. A. Arsenault, N. J. Cullen, and K. Steffen (2002), Vertical fluxes of NO<sub>x</sub>, HONO, and HNO<sub>3</sub> above the snowpack at Summit, Greenland, *Atmos. Environ.*, *36*, 2629–2640.
- Jacobson, M. Z. (2004), Climate response of fossil fuel and biofuel soot, accounting for soot's feedback to snow and sea ice albedo and emissivity, *J. Geophys. Res.*, *109*, D21201, doi:10.1029/2004JD004945.
- King, M. D., and W. R. Simpson (2001), Extinction of UV radiation in Arctic snow at Alert, Canada (82 degrees N), *J. Geophys. Res.*, *106*(D12), doi:10.1029/2001JD900006.
- Kirchstetter, T. W., T. Novakov, and P. V. Hobbs (2004), Evidence that the spectral dependence of light absorption by aerosols is affected by organic carbon, *J. Geophys. Res.*, *109*, D21208, doi:10.1029/2004JD004999.
- Koch, D., S. Menon, A. Del Genio, R. Ruedy, I. Alienov, and G. A. Schmidt (2009), Distinguishing aerosol impacts on climate over the past century, *J. Climate*, *22*(10), 2659–2677, doi: 10.1175/2008jcli2573.1.
- Millikan, R. C. (1961), Optical properties of soot, *J. Opt. Soc. Am.*, *51*, 698–699.
- Ming, J., C. Xiao, H. Cachier, D. Qin, X. Qin, Z. Li, and J. Pu (2009), Black carbon (BC) in the snow of glaciers in west China and its potential effects on albedo, *Atmos. Res.*, *92*, 114–123, doi:10.1016/j.atmosres.2008.09.007.
- Østrem, G. (1959), Ice melting under a thin layer of moraine, and the existence of ice cores in moraine ridges, *Geogr. Ann.*, *41*, 228–230.
- Painter, T. H., A. P. Barrett, C. C. Landry, J. C. Neff, M. P. Cassidy, C. R. Lawrence, K. E. McBride, and G. L. Farmer (2007), Impact of disturbed desert soils on duration of mountain snow cover, *Geophys. Res. Lett.*, *34*, L11502, doi:10.1029/2007GL030284.
- Painter, T. H., A. C. Bryant and S. M. Skiles (2012), Radiative forcing by light absorbing impurities in snow from MODIS surface reflectance data, *Geophys. Res. Lett.*, *39*, L17502, doi:10.1029/2012GL052457.
- Perovich, D. K., T. C. Grenfell, B. Light, and P. V. Hobbs (2002), Seasonal evolution of the albedo of multiyear Arctic sea ice, *J. Geophys. Res.*, *107*(C10), 8044, doi:10.1029/2000JC000438.
- Reay, H. J., J. L. France, and M. D. King (2012), Decreased albedo e-folding depth and photolytic OH radical and NO<sub>2</sub> production with increasing black carbon content in Arctic snow, *J. Geophys. Res.*, *117*, D00R20, doi: 10.1029/2011JD016630.
- Rhodes, J. J., R. L. Armstrong, and S. G. Warren (1987), Mode of formation of “ablation hollows” controlled by dirt content of snow, *J. Glaciol.*, *33*, 135–139.
- Roden, C. H., T. C. Bond, S. Conway, and A. B. Osorto Pinel (2006), Emission factors and real-time optical properties of particles emitted from traditional wood burning cook stoves, *Environ. Sci. Technol.*, *40*, 6750–6757.
- Rosen, H., A. D. A. Hansen, L. Gundel, and T. Novakov (1978), Identification of the optically absorbing component in urban aerosols, *Appl. Opt.*, *17*, 3859–3861.
- Rypdal, K., N. Rive, T. K. Berntsen, Z. Klimont, T. K. Mideksa, G. Myhre, and R. B. Skeie (2009), Costs and global impacts of black carbon abatement strategies, *Tellus B*, *61*(4), 625–641, doi: 10.1111/j.1600-0889.2009.00430.x.
- Skeie, R. B., T. Berntsen, G. Myhre, C. A. Pedersen, J. Ström, S. Gerland, and R. A. Ogren (2011), Black carbon in the atmosphere and snow, from pre-industrial times until present, *Atmos. Chem. Phys.*, *11*, 6809–6836, doi: 10.5194/acp-11-6809-2011.
- Sun, H., L. Biedermann, and T. C. Bond (2007), Color of brown carbon: A model for ultraviolet and visible light absorption by organic carbon aerosol, *Geophys. Res. Lett.*, *34*, L17813, doi:10.1029/2007GL029797.
- Wang, X., S. J. Doherty, and J. Huang (2013), Black carbon and other light-absorbing impurities in snow across Northern China, *J. Geophys. Res.*, doi:10.1029/2012JD018291.
- Warren, S. G. (1984), Impurities in snow: Effects on albedo and snowmelt, *Ann. Glaciol.*, *5*, 177–179.
- Xu, B., T. Yao, X. Liu, and N. Wang (2006), Elemental and organic carbon measurements with a two-step heating gas chromatography system in snow samples from the Tibetan Plateau, *Ann. Glaciol.*, *43*, 257–262, doi: 10.3189/172756406781812122.
- Xu, B., et al. (2009), Black soot and the survival of Tibetan glaciers, *Proc. Natl. Acad. Sci. USA*, *106*(52), 22114–22118, doi: 10.1073/pnas.0910444106.
- Xu, B., J. Cao, D. R. Joswiak, X. Liu, H. Zhao, and J. He (2012), Post-depositional enrichment of black soot in snow-pack and accelerated melting of Tibetan glaciers, *Environ. Res. Lett.*, *7*, doi:10.1088/1748-9326/7/014022.